

# Volcanic facies architecture of an intra-arc strike-slip basin, Santa Rita Mountains, Southern Arizona

Cathy J. Busby · Kari N. Bassett

Received: 10 December 2002 / Accepted: 8 February 2006 / Published online: 31 March 2007  
© Springer-Verlag 2007

**Abstract** The three-dimensional arrangement of volcanic deposits in strike-slip basins is not only the product of volcanic processes, but also of tectonic processes. We use a strike-slip basin within the Jurassic arc of southern Arizona (Santa Rita Glance Conglomerate) to construct a facies model for a strike-slip basin dominated by volcanism. This model is applicable to releasing-bend strike-slip basins, bounded on one side by a curved and dipping strike-slip fault, and on the other by curved normal faults. Numerous, very deep unconformities are formed during localized uplift in the basin as it passes through smaller restraining bends along the strike-slip fault. In our facies model, the basin fill thins and volcanism decreases markedly away from the master strike-slip fault (“deep” end), where subsidence is greatest, toward the basin-bounding normal faults (“shallow” end). Talus cone-alluvial fan deposits are largely restricted to the master fault-proximal (deep) end of the basin. Volcanic centers are sited along the master fault and along splays of it within the master fault-proximal (deep) end of the basin. To a lesser degree, volcanic centers also form along the curved faults that form structural highs

between sub-basins and those that bound the distal ends of the basin. Abundant volcanism along the master fault and its splays kept the deep (master fault-proximal) end of the basin overfilled, so that it could not provide accommodation for reworked tuffs and extrabasinally-sourced ignimbrites that dominate the shallow (underfilled) end of the basin. This pattern of basin fill contrasts markedly with that of nonvolcanic strike-slip basins on transform margins, where clastic sedimentation commonly cannot keep pace with subsidence in the master fault-proximal end. Volcanic and subvolcanic rocks in the strike-slip basin largely record polygenetic (explosive and effusive) small-volume eruptions from many vents in the complexly faulted basin, referred to here as multi-vent complexes. Multi-vent complexes like these reflect proximity to a continuously active fault zone, where numerous strands of the fault frequently plumb small batches of magma to the surface. Releasing-bend extension promotes small, multivalent styles of volcanism in preference to caldera collapse, which is more likely to form at releasing step-overs along a strike-slip fault.

**Electronic supplementary material** The online version of this article (doi:10.1007/s00445-007-0122-9) contains supplementary material, which is available to authorized users.

Editorial responsibility: J. Donnelly-Nolan

C. J. Busby (✉)  
Department of Geological Sciences, University of California,  
Santa Barbara, CA 93106, USA  
e-mail: busby@geol.ucsb.edu

K. N. Bassett  
Department of Geological Sciences, University of Canterbury,  
Prvt. Bag 3800, Christchurch, New Zealand  
e-mail: kari.bassett@canterbury.ac.nz

**Keywords** Intra-arc · Strike-slip basin · Volcanic facies architecture · Glance Conglomerate · Polygenetic · Multi-vent

## Introduction

Facies architectural models have been developed to a sophisticated degree for the sedimentary fill of strike-slip basins along conservative plate margins (Nilsen and Sylvester 1995; Holdsworth et al. 1998; Barnes and Audru 1999; Barnes et al. 2001; Link 2003). There remains, however, a complete lack of volcanic facies architectural models for

strike-slip basins along convergent margins, probably due to additional complexities inherent in volcanic facies analysis, including abrupt lateral facies changes, and postdepositional modification by intrusive and hydrothermal activity. Although less can generally be learned about the details of eruption, transport and depositional processes in ancient volcanic successions relative to modern volcanoes, more can be learned about processes that act over long time scales (e.g. millions of years), and how these processes influence the final product in the volcanic rock record.

Strike-slip faults are common in modern and ancient arc terranes, but their effects have been much better studied in arc basement rocks (plutonic and metamorphic) than they have been in arc volcanic rocks. Oblique convergence is far more common than orthogonal convergence, and at most continental arcs, an obliquity of only 10° off orthogonal results in the formation of strike-slip faults in the upper plate (Fitch 1972; Jarrard 1986a; McCaffrey 1992). These faults commonly form in the thermally weakened crust of the arc, particularly on continental crust, which is weaker and better coupled to the subducted slab than oceanic-arc crust (Dewey 1980; Jarrard 1986a; Ryan and Coleman 1992; Smith and Landis 1995). Strike-slip faults, transtensional faults, and block rotations play an important role in modern volcanic arcs; examples include the Central American arc (Burkhart and Self 1985; Jarrard 1986b; Weinberg 1992); the Trans-Mexican Volcanic belt (Israde-Alcantara and Garduno-Monroy 1999); the Andean arc of southern Chile and Patagonia (Cembrano et al. 1996; Thomson 2002); the Sumatra arc (Bellier and Sebrier 1994); the Aeolian arc (Gioncada et al. 2003); the Calabrian arc (Van Dijk 1994); the Aleutian arc (Geist et al. 1988); the Taupo Volcanic Zone (Cole and Lewis 1981); the central Philippine arc (Sarewitz and Lewis 1991); and others. Strike-slip basins are the most tectonically active type of basin (Nilsen and Sylvester 1995), so the effects of strike-slip faulting on the development of volcanic successions within arcs must be profound.

In this paper, we show how the three-dimensional arrangement of volcanic deposits (“facies architecture”) in strike-slip basins is not only the product of volcanic processes, but also of tectonic processes. We do this by describing and interpreting the largely volcanic fill of an intra-arc strike-slip basin that is very well exposed in cross-sectional view (Figs. 1 and 2). This basin is preserved within the Jurassic arc of southern Arizona, and its fill is the Santa Rita Glance Conglomerate (as defined by Bassett and Busby 2005). The volcanology and volcanic facies architecture of this intra-arc strike-slip basin was not only controlled by volcanic eruptive and depositional processes, but also by tectonic processes. These include structural controls on patterns of uplift and subsidence, on locations of vents, and on types of centers that develop.

From our work on this ancient intra-arc basin, we develop a facies architectural model for a volcanically-dominated releasing-bend basin along a strike-slip fault. Modern analogs show that these basins have the highest preservation potential along strike-slip faults with a component of transtension, where subsidence at releasing bends is greater than uplift at restraining bends (e.g. Cowan et al. 1989; Cowan and Pettinga 1992). As a basin slips through multiple releasing and restraining bends, it develops a thick basin fill cut by numerous deep unconformities. The resulting “releasing-and-restraining bend basin” has a very distinctive volcanic facies architecture.

### Geologic setting

Late Jurassic strike-slip intra-arc basins formed along the axis of earlier Early to Middle Jurassic extensional intra-arc basins on continental crust in southern Arizona (Fig. 1; Busby et al. 2005). The Sawmill Canyon fault zone formed the north-eastern boundary of the Early to Middle Jurassic extensional arc graben depression (Busby-Spera 1988; see “Jurassic volcanic rocks,” Fig. 1). Then Late Jurassic intra-arc strike-slip basins developed along Sawmill Canyon fault zone, which we infer was an inboard strand of the sinistral Mojave-Sonora megashear system (Busby et al. 2005). The fill of the intra-arc strike-slip basins is dominated by volcanic rocks but also contains abundant conglomerate (“Glance Conglomerate with interbedded volcanic rocks,” Fig. 1). These contrast with basins to the east, or inboard (backarc) with respect to the subduction margin, which have little or no volcanic fill (“Glance Conglomerate without interstratified volcanic rocks”, Fig. 1). Lawton and McMillan (1999) use geochemical data on sparse mafic volcanic rocks of the eastern Glance Conglomerate belt to infer a rift tectonic setting. Volcanic rocks of the western Glance Conglomerate, in contrast, show many features typical of arcs (Busby et al. 2005; Bassett and Busby 2005). This paper focuses on rhyolitic, dacitic and andesitic arc volcanic rocks and interstratified conglomerates along the Sawmill Canyon fault zone in the Santa Rita Mountains (Figs. 1 and 2), referred to as the Santa Rita Glance Conglomerate (Bassett and Busby 2005).

The Santa Rita Glance Conglomerate crops out in a 20 × 6.5 km elongate belt extending southward from the Sawmill Canyon strike-slip fault zone (Fig. 2). Beds strike roughly north and dip ~30°E, producing an oblique cross-section in map view that lies at ~55° angle to the NW–SE strike of the fault zone (Fig. 2). The Santa Rita Glance Conglomerate lies unconformably on Middle Jurassic volcanic, sedimentary, and granitic rocks that formed in an extensional continental arc setting (Busby-Spera 1988; Riggs and Busby-Spera 1990; Busby et al. 2005). The top of the Santa Rita Glance Conglomerate is cut by splays of the

Sawmill Canyon fault zone to the northeast, and it is buried by Quaternary gravels to the southeast (Fig. 2).

In the following section, we present a volcanic lithofacies map and descriptions (Fig. 2, Table 1), outcrop photos (Figs. 3, 4, 5 and 6) and measured sections (ESM) of the Santa Rita Glance Conglomerate, in order to interpret eruptive and depositional processes, by analogy with the deposits of modern volcanoes. This is followed by a discussion of strike-slip basins, and presentation of a facies architectural model that describes the controls of syn-depositional faults and deep unconformities on the distribution of vents and volcanic lithofacies in an intra-arc strike-slip basin.

**Lithofacies and lithofacies associations**

Most of the lithofacies of the Santa Rita Glance Conglomerate (Table 1) are repeated at several stratigraphic levels (Figs. 2; ESM), separated by multiple unconformities and syn-depositional faults (Fig. 2). Volcanic terminology follows that of Fisher and Schmincke (1984), Heiken and Wohletz (1985), and Sigurdsson et al. (2000). The following descriptions and interpretations were made based on detailed lithofacies mapping (Fig. 2) and petrographic study of ~400 thin sections, and limited geochemical analysis (Bassett and Busby 2005). See Table 1 for full descriptions and interpretations of each rock type in the order presented below.

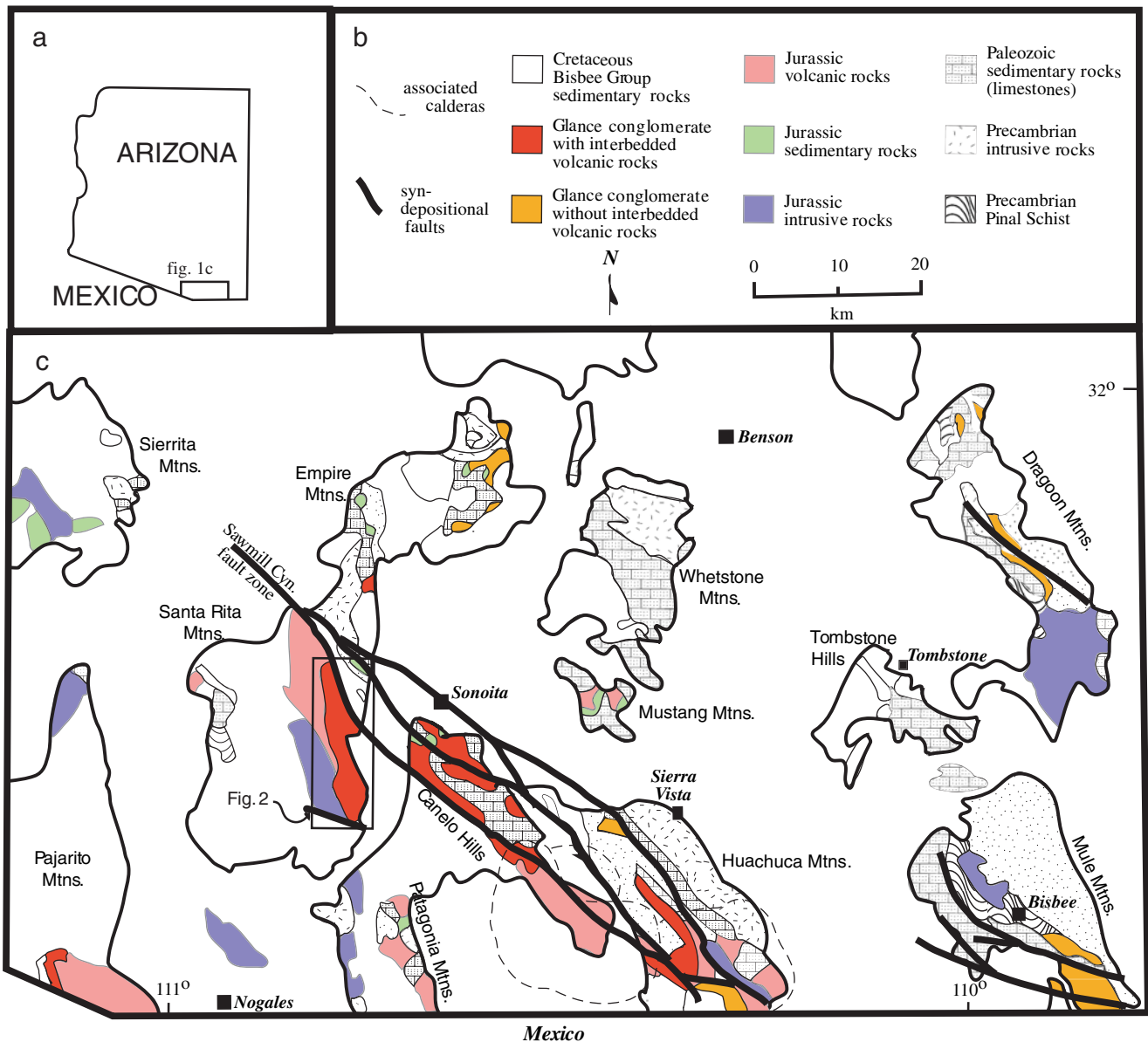


**Fig. 1** Location and geologic setting of the Glance Conglomerate in the Santa Rita Mountains, southern Arizona, compiled from numerous publications cited by Busby et al. (2005)

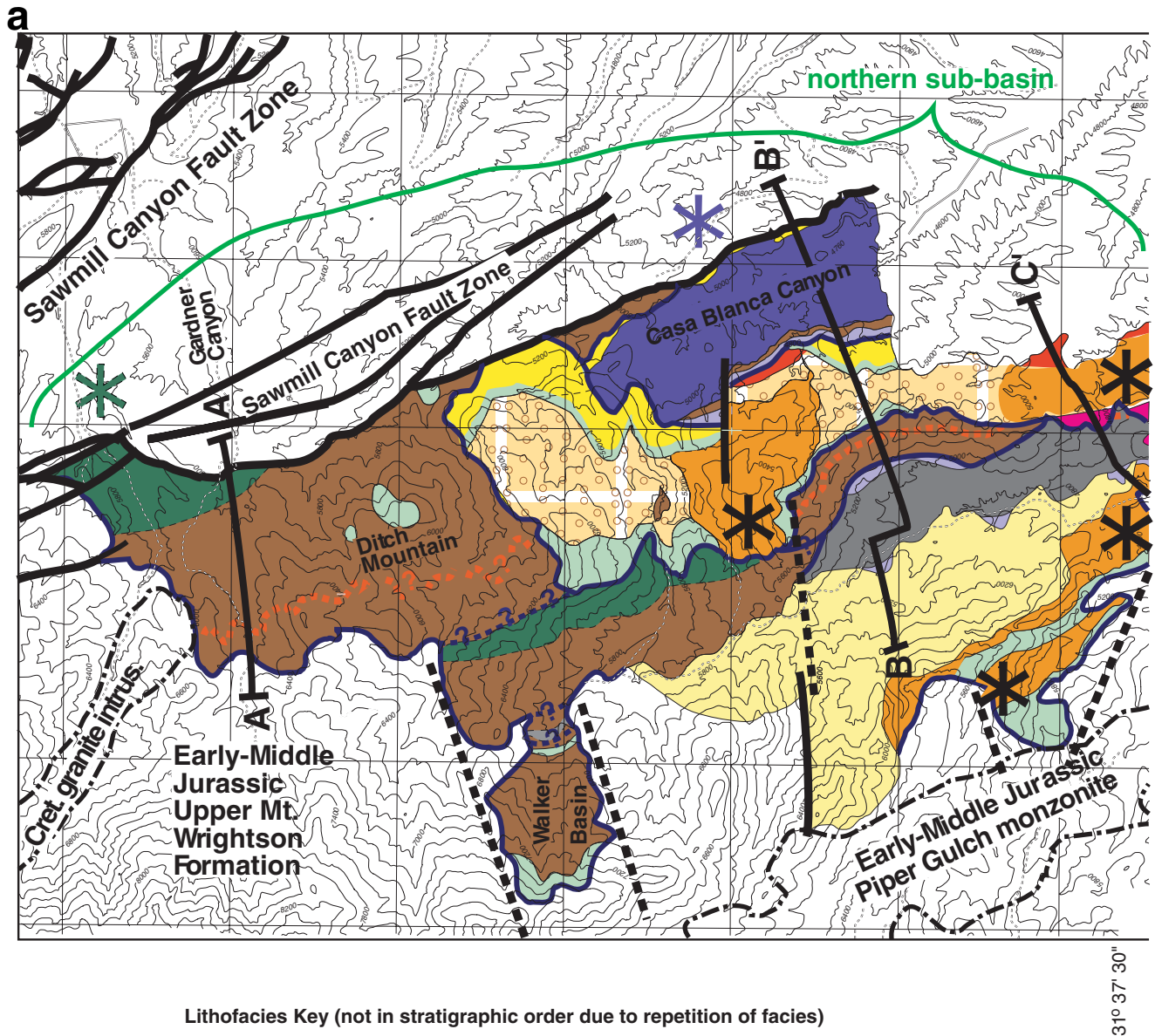
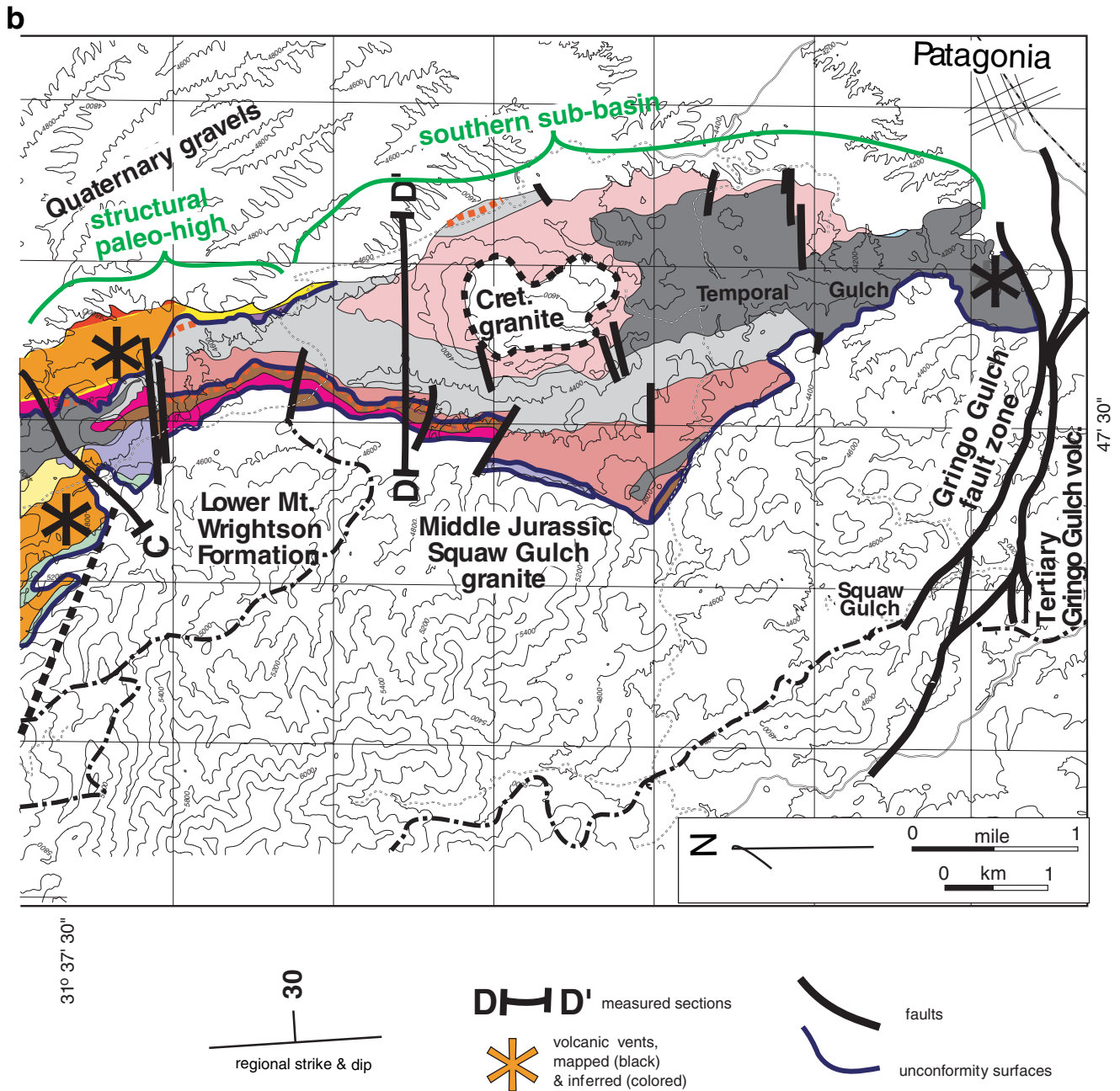


**Fig. 2** Lithofacies map of the Glance Conglomerate in the Santa Rita Mountains of southern Arizona (note north is to left of the two pages). The strike and dip of the homoclinal section allows an oblique cross-sectional view of the basin fill. The basin is bounded to the north by the regionally significant Sawmill Canyon fault zone, which extends southward through the Huachuca Mountains into Mexico (Fig. 1); this

forms the master fault to the basin while a localized, subordinate fault zone (Gringo Gulch) bounds the basin to the south. A paleo-high formed by high-angle faults divides the basin into a northern sub-basin proximal to the master fault (measured sections A, B, C, *ESM*) and a southern sub-basin distal to the master fault (measured section D, *ESM*)



Fig. 2 (continued)



**Boulder breccia-conglomerate**

Although the Glance Conglomerate contains well-rounded clasts at some localities in southern Arizona, at others it is composed almost entirely of angular clasts (Klute 1991). In the Santa Rita Glance Conglomerate, the “conglomerate” is almost all angular (Fig. 3), and only granitic clasts are locally subrounded, probably as they were weathered from

the outcrop. For this reason, we refer to it as “breccia-conglomerate.” The boulder breccia-conglomerate is largely interstratified with dacitic block-and-ash-flow tuffs adjacent to the Sawmill Canyon fault zone, although it interfingers with other lithofacies further from the fault zone (Fig. 2). The matrix of the boulder breccia-conglomerate ranges from dacitic where it interfingers with dacitic block-an-ash-flow tuffs, to arkosic sandstone, derived from erosion of extra-

**Table 1** Table of lithofacies descriptions and interpretations

ROCK NAME	SPATIAL DISTRIBUTION	FIELD CHARACTERISTICS	THIN SECTION CHARACTERISTICS	FACIES INTERPRETATION	ANALOGS WITH REFERENCES
<b>boulder breccia-conglomerate</b>	Thickens and coarsens dramatically toward the master fault (Sawmill Canyon fault zone).	Massive coarse-grained boulder breccia-conglomerate (D99=7–8 m, D90=2–3 m, D50=60 cm); polymict, very angular to sub-rounded clasts of local derivation. <b>TALUS DEPOSITS</b> - tightly-packed, angular to subrounded clasts with <10% infiltrated sand matrix, lacking stratification or sorting. <b>PROXIMAL DEBRIS-FLOW DEPOSITS</b> - matrix-supported boulder-to pebble-sized clasts; no sorting or clast alignment. <b>MEDIAL TO DISTAL DEBRIS FLOW DEPOSITS</b> - crudely-stratified matrix-supported boulder to pebble breccia-conglomerate with flat clast alignment. <b>STREAMFLOW DEPOSITS</b> - moderately well-sorted, stratified and cross stratified granule sandstone with lenses of pebble- to boulder-conglomerate.	<b>ARKOSIC SANDSTONE MATRIX</b> - granite lithics & few silicic volcanics & xls. of kspar, qtz., microcline > biotite, plag. <b>DACITIC LITHIC TUFF MATRIX</b> - f.g. dacite or rhyolite volcanic lithics & xls. of plag. > qtz. <b>RHYOLITIC LAPILLI TUFF MATRIX</b> - shards, pumice, qtz., volcanic lithics.	Shed from Sawmill Canyon fault zone on surfaces of great relief. Talus breccia & avalanche deposition within ~100 m of the fault scarp; Proximal to medial debris flow deposition within 3 km of fault zone; Distal sheetwash & channelized stream flow within 5 km of fault zone. <b>MATRIX COMPOSITION</b> determined by availability of volcanic material.	Talus cones that passed basinward into steep-sided, very coarse-grained fans almost entirely deposited from debris flows, like those described by Collinson (1996). Sedimentologically (but not compositionally) similar to the Violin Breccia, deposited along a precursor of the San Andreas Fault (Crowell, 1982; Link, 2003).
<b>dacitic block &amp; ash flow tuffs</b>	Restricted to master fault-proximal sub-basin, thickens and coarsens dramatically toward master fault.	Greenish-gray, massive, matrix supported, poorly-sorted monomict tuff breccia and lesser lapilli tuff (D90<1 m, D50~10–30 cm or D90=30 cm, D50<5 cm). Clasts of angular, nonvesiculated (dense) dacitic blocks in a matrix of lapilli-to ash-sized fragments of the same composition and shape. Rare plastically deformed "amoeboid" (nonvesicular) clasts. Pumice and bubble-wall shards entirely absent. No associated intrusions or lava flows.	70 - 85% dense dacite clasts and 15–30% crystals of plag>>qtz = biotite with rare hb.	Dacitic block-and-ash flows generated by gravitational lava dome collapse along the master fault basin margin. Coarse grain size and (rare) occurrence of amoeboid clasts appear proximal, but lack of lava flow/intrusive equivalents in basin suggest extrabasinal source, probably dome(s) plumbed up the master fault.	Small-volume pyroclastic flows associated with dome collapse (e.g. Fisher et al., 1980; Sparks, 1997; Freundt et al., 2000). Similar to deposits described at Unzen volcano (Miyabuchi, 1999; Nakada et al., 1999; Ui et al., 1999).
<b>andesitic lava flows, flow breccias &amp; intrusions</b>	Vented along the master fault and its splays, along the structural high between sub-basins, and at the fault-bounded distal end of the basin.	Dark gray to black; generally coherent with large plag. xls., commonly flow aligned; locally flow banded, brecciated & vesicular. <b>LAVA FLOWS</b> are conformable with stratigraphy, with or without flow-top breccias. <b>INTRUSIONS</b> are largely coherent, generally nonvesiculated units that, at least locally, cross-cut stratigraphy and generally have a higher crystal content than the lava flows. Sills and flows commonly difficult to distinguish and are mapped as a single unit.	10–50% phenocrysts., mostly plagioclase, tr.-3% amphibole, <5% Cpx, 3% tr. Apatite in microcrystalline to holocrystalline groundmas. Rare granite accidental lithics introduce Kspar, qtz., titanite.	Flow banding, flow-aligned crystals, and flow breccias typical of intermediate-composition volcanic rocks. Features typical of mafic flows and vents (see Self et al., 1997; Cashman et al. 2000; Hon et al., 2002) are absent.	The thicknesses of the intrusions, their limited lateral extent, and the alternation of sills with brecciated lava flows indicate emplacement as sill-like bodies that intruded early-erupted flows and vented locally to feed more lava flows (Fisher and Schmincke, 1984; Fink and Anderson, 2000).
<b>andesitic ignimbrite</b>	Underlying andesitic lava flows or vulcanian breccia.	Dark lavender to purple-red, xl. rich, massive, lapilli tuff with abundant flattened scoria and minor cognate lithic fragments in an unsorted matrix of bubble-wall shards. Thicknesses from ~2 m to up to 10 m adjacent to syn-depositional faults. Generally nonwelded with one showing localized welding.	35–40% crystals (plag>>biotite), flattened scoria and bubble-wall shards; the welded one is less xl.-rich (10–15%).	Andesitic pumice-rich pyroclastic flows (Fisher and Schmincke, 1984; Freundt et al., 2000), largely non-welded. Three of the four andesitic ignimbrites occur at the bases of andesitic lava flow or vulcanian breccia sequences and may represent the first, degassing phase of the andesitic eruptions (Fisher and Schmincke, 1984).	Intermediate-composition ignimbrites are less common than silicic ones, but have been reported from the Andean arc (McCurry and Schmidt, 2001) the Aleutian arc (Larsen et al., 2000), the Roman Volcanic province (Giordano et al., 2002), Java (Camus et al., 2000) and the Taupo Volcanic Zone (Wilson et al., 1995).
<b>andesitic vitric tuff &amp; tuffaceous sandstone</b>	Restricted to master fault-distal sub-basin.	Dark purplish-grey to purplish black <b>VITRIC TUFF TO TUFFACEOUS VOLCANIC LITHIC SANDSTONE</b> : very poorly sorted, dark colored tuff OR tuffaceous sandstone; largely massive to indistinctly stratified in medium to very thick beds (up to 15 m thick); lesser convolute lamination, planar lamination and cross lamination. Scattered small scours (~1–2 m wide) filled with arkose-matrix boulder breccia-conglomerate.	<b>VITRIC TUFF</b> - ~90% shards & scoria shreds, dominantly bubble wall but also platy, blocky, & splintery shards; 10% andesite lithics; euhedral xls. of plag., biotite <b>TUFFACEOUS VOLCANIC LITHIC SANDSTONE</b> - >75% andesitic lithics of varying vesicularity and crystal content in a crystal vitric tuff matrix with squashed scoria shreds. Euhedral to subrounded xls. of plag. >> biotite >> qtz. > hb.	Fluvial reworking of andesitic pyroclastic (Fisher and Schmincke, 1984) and phreatomagmatic (Heiken and Wohletz, 1985; McPhie et al., 1993) tephra. Abundance of delicate pyroclastic material indicates proximal deposition, likely from intrabasinal sources, and availability of running water. Intercalated arkosic breccia-conglomerate record "background sedimentation" from fault scarps when the basin was not overwhelmed by the local andesitic source.	Very poorly sorted and indistinctly stratified texture of the vitric tuffs/tuffaceous sandstone indicates deposition from hyperconcentrated flood flow and nonchannelized overland flow (Smith and Lowe, 1991; Collinson, 1996; Allen, 1997; Vallance, 2000). Convolute lamination indicates soft-sediment deformation of water-saturated sediment (Reineck and Singh, 1980), probably reflecting high sedimentation rates.
<b>andesitic vulcanian breccia</b>	Forms a single, 500 m thick sequence within a kilometer of the master fault; vent inferred to have been sited along the master fault.	Dark gray to black, monomict clast-supported breccia composed of dense and rigid, angular crystal-rich andesitic blocks up to 1 m, and lesser nonjuvenile fragments of granitic rock and silicic volcanic rock. Less than 25% ash matrix, composed of monolithic andesite rock fragments of the same composition as the blocks, as well as lesser nonjuvenile clasts. In multi-meter to decameter thick, massive to crudely normally graded beds, in places cut by scours containing fluvial lag deposits of granite boulders	xl. rich (30–40%) with 30% plag., 5% biotite, <3% hb; mafics generally altered to oxides; dense juvenile lithics and lesser accidental rock fragments.	Proximal, ponded accumulations from andesitic vulcanian eruptions (Gourgaud et al., 2000) - moderate to violent ejection of solid fragments of high density juvenile clasts (Heiken and Wohletz, 1985) and nonjuvenile fragments torn from the vent walls or cap rock. Uniformly coarse grain size, clast-supported texture and crude stratification formed by ballistic ejection in discrete, small-volume, closely-spaced explosions (Melson and Saenz, 1973; Nairn and Self, 1978). Lack of block and ash flow	Eruptions triggered by overpressuring under a caprock or plug of solidified material in the throat of a vent, by decompression of a conduit during lava dome collapse, or by magma interaction with water, either surface or groundwater (Nairn and Self, 1978; Self et al., 1979; Wilson, 1980; Francis, 1993; Stix et al., 1997; Morrissey and Mastin, 2000; Druitt et al., 2002). High crystallinity may inhibit bubble expansion (Cashman et al.,

Table 1 (continued)

				tuff interbeds indicates that the ballistics did not feed mobile avalanches, perhaps because they were ponded in a basin near the vent, which also explain their great thickness. Historic vulcanian eruptions also include minor andesite ignimbrite/ash-and-scoria flows (Camus et al., 2000; Druitt et al., 2002) like one that lies downsection (Fig 2).	2000). Modern block fields lie within about five kilometers of their vents (Yamagishi and Freebrey, 1994; Morrissey and Mastin, 2000; Gourgaud et al., 2000).
<b>rhyolitic intrusions</b>	Feeders to six lava domes, following faults.	White, nearly aphyric, coherent, faintly flow-banded bodies that crosscut stratigraphy with very irregular contacts, and appear altered.	xl. poor 5-10% tot. of Kspar or plag. >qtz in a microcrystalline groundmass with shadowy, indistinct flow banding; more altered (with quartz and optically irresolvable clay minerals) than extrusive equivalents.	Shallow-level intrusions that supplied magma to intrabasin domes upsection. Vent locations were fault controlled.	
<b>rhyolitic dome &amp; dome breccias</b>	Six lava domes sited on faults, all within the master fault-proximal sub-basin or on the structural high between the sub-basins.	White, nearly aphyric flow-banded coherent rhyolite mantled by breccia of the same composition. Form bodies 0.5 to 2 km in diameter and ~100 m to ~500 m thick. Rest upon intrabasin faults. Block size in carapace decreases away from coherent cores, from 2 to 0.2 m in diameter. Breccias are clast-supported and monomict, except for local occurrences of pink, very fine-grained, well sorted, vitric tuff in thin, discontinuous lenses.	Very xl. poor to aphyric ~5% tot. of plag. or ksp. tr. qtz., tr. biotite; f.g. qtz.-fld. mosaic matrix; flow banding common; rare granite accidentals may introduce kspar.	Rhyolitic lava domes with flow banding; coherent interiors mantled by breccias in gradational, complexly interfingering contact, showing systematic decrease in block size with distance away from the vent. Formed along intrabasin faults, which acted as conduits for the rhyolitic intrusions.	Endogenous domes, based on their small size, blocky carapace, and bulbous shape with little evidence for extensive lateral flow away from the vent and (Fink and Anderson, 2000). Relatively small block sizes suggest high extrusion rates (Fink and Anderson, 2000). Pink porcellanite lenses indicate intermittent phreatoplinian explosive eruptions (Morrissey et al., 2000).
<b>rhyolitic block &amp; ash flow tuffs</b>	Fringe the lava dome-dome breccia lithofacies with gradational contacts.	White to pink, monomict tuff breccia in matrix-supported, massive beds 5-30 m thick. Angular clasts ~5-30 cm, nonvesiculated to poorly-vesiculated; pumice very rare.	Mineralogy same as dome breccias; dense clasts in a vitriclastic matrix.	Rhyolitic block-and-ash-flows generated by collapse of oversteepened domes.	Same as dacite block-and-ash flow tuffs.
<b>rhyolitic crystal-poor ignimbrites</b>	Interstratified with rhyolitic dome breccias or rhyolite plinian-phreatoplinian tuffs.	Abundant white pumice, commonly flattened, in a pink to white aphyric matrix of vitric tuff, in massive beds 1 - 20 m thick. Filling scours with 20-40 cm relief. Locally contain <1 m thick beds with sorting, stratification and cross-stratification.	xl. poor to aphyric <5% tot. of plag., tr. biotite, tr. qtz., tr. Kspar, in unwelded matrix of shards & pumice, local lithics. Shards dominantly blocky or splintery, with lesser bubble wall.	Phreatoplinian ignimbrite, based on highly pumiceous, massive, poorly sorted nature (Sparks et al., 1973; Fisher and Schmincke, 1984), combination of blocky, splintery and bubble-wall shards, and lack of welding (Heiken and Wohletz, 1985; McPhie et al., 1993; De Rita et al., 2002). Vent-proximal deposits with weakly erosive basal contacts (Freundt et al., 2000). Availability of water also indicated by local fluvial reworking	Interstratification with phreatoplinian tuffs supports phreatoplinian ignimbrite interpretation (Bryan et al., 2000; De Rita et al., 2002). Lack of accretionary lapilli attributed to poor preservation potential, since accretionary lapilli are uncommon (Self, 1983; Houghton et al., 2000b) to absent (Bryan et al., 2000) from young unaltered phreatoplinian ignimbrites.
<b>rhyolitic, white, high-grade ignimbrite</b>	Single unit, overlies two rhyolite domes; incompletely preserved.	White, aphyric moderately-welded pumice lapilli tuff, tens of meters thick, with well-preserved vitroclastic textures, containing several ultrawelded horizons. Ultrawelded horizons show lineations on planar to highly contorted parting surfaces; at one locality it contains aligned tubes 10-20 cm in diameter and 1-2 m long infilled with quartz crystals.	aphyric to xl. poor ~5% tot. of <5% plag., <1% qtz., <1% biotite; ultrawelded horizons show extreme plastic deformation of shards and stretching of pumice; moderately welded horizons show sintering of shards and moderate flattening of pumice; bubble-wall shards only, no blocky or splintered shards.	Rhyolitic ignimbrite, moderately welded to very strongly welded, with multiple cooling units, suggesting either fluctuation in the eruptive column or multiple ignimbrite emplacement. Welding and absence of blocky shards indicate "dry" eruption. Subparallel, linear tubes in the high-grade ignimbrites may record quenching against logs.	High grade ignimbrites, formed by primary deformation of high-temperature pyroclastic flows during transport and deposition (Branney and Kokelaar, 1992; McCurray et al., 1996; Freundt, 1999) or secondary rheomorphic flowage after deposition and deflation (Schmincke and Swanson, 1967; Wolff and Wright, 1981).
<b>rhyolitic crystal-rich ignimbrites</b>	In master fault-distal sub-basin, onlapping paleo-structural high (two units)	White, massive tuff with fiamme and large qtz. & biotite xls.; top locally more pumiceous.	30-35% xls up to 4 mm in size, tot. of 15% qtz., 10% plag., 5% biotite, <2% kspar; non-welded bubble wall shards & pumice.	Silicic crystal & pumice rich pyroclastic flow, non-welded	Ignimbrites, based on highly pumiceous, massive, poorly sorted nature (Sparks et al., 1973; Fisher and Schmincke, 1984).
<b>rhyolitic lithic-rich ignimbrite</b>	In master fault-distal sub-basin, onlapping paleo-structural high (one unit).	White, massive pumice lapilli tuff, with abundant lithic fragments (~20-30%) of white tuff, red andesite, siltstone, granite, D99=2 m, D90=20-50cm, D50=5 cm.	<15% xls, plag>>qtz.>Kspar, well-preserved nonwelded vitriclastic texture of pumice shreds & bubble wall shards; lithics ~20-30%.	Silicic lithic & pumice rich pyroclastic flow, non-welded.	Ignimbrite.
<b>rhyolitic limestone lithic ignimbrite</b>	Restricted to master fault-distal sub-basin (one unit).	White to light lavender, massive, crystal-poor pumice lapilli tuff with four welded horizons; lithics range from limestone to marble to amphibolite depending on degree of welding.	5-13% xls, tot of 10% plag., 3% biotite, tr. qtz.; plag. often completely altered to calcite; bubble wall shards and pumice.	Silicic pumice-rich welded to nonwelded pyroclastic flows bearing distinctive carbonate clasts of extrabasin origin.	Multiple cooling units suggest instability in the eruptive column or multiple ignimbrite emplacement (Freundt et al., 2000).
<b>rhyolitic, red, high-grade</b>	Lower unit restricted to master fault-	Red-maroon ultrawelded ignimbrites, each only a few meters thick; xl. poor with plag. only. Upper higher unit is a spherulitic	xl. poor <5% tot. of ~5% plag., tr. biotite>qtz.; more xl. rich in nonwelded	Silicic pumice rich pyroclastic flows, largely ultrawelded "lava like" ignimbrite. Distinguished from lava	High-grade ignimbrites (see discussion of white, rhyolitic high-grade ignimbrite, above),

**Table 1** (continued)

<b>ignimbrites</b>	distal (southern) sub-basin, but erosional remnants of the upper unit occur across both sub-basins.	and locally brecciated ignimbrite for ~7 km distance, passing laterally into a single layer of 2–3 m blocks for another ~4.5 km (within boulder breccia-conglomerate).	outcrop ~15% tot.; vitriclastic texture of faint fiamme in highly welded samples to bubble wall shards in nonwelded samples; locally spherulitic, hematized; rare vesicles.	flows by preservation of basal welding or nonwelded textures at some localities (e.g. see Henry and Wolff, 1992; Milner et al., 1992; Kirstin et al., 2001). The large blocks that extend in a single layer 4.5 km across the basin were likely shed from/reworked from the upper lava-like ignimbrite.	with hot-state brecciation occurred during rheomorphic flow in the late stages of cooling (Branney and Kokelaar, 1992, 1994; Beddoe-Stephens and Millward, 2000).
<b>rhyolite plinian and phreato-plinian tuffs</b>	Widespread.	In order of abundance: <i>PLINIAN PUMICE FALL DEPOSITS</i> - light greenish-white, nonwelded pumice beds that mantle topography. <i>REWORKED PLINIAN FALL DEPOSITS</i> - medium-bedded, erosively-based, lenticular, locally cross-laminated pumice lapillistones with more rock fragments and less glass than fall deposits. <i>PHREATOPLINIAN FALL DEPOSITS</i> - pinkish red porcellanite in thin to very thin tabular beds that mantle topography, with convolute lamination.	<i>PLINIAN PUMICE FALL DEPOSITS</i> - ~80–90% pumice shreds (some long tube), 10–20% bubble-wall shards, aphyric to xl poor. <i>REWORKED</i> - enriched in crystals and accidental rocks fragments. <i>PHREATO-PLINIAN FALL DEPOSITS</i> - >80–90% blocky shards; remainder irresolvably fine grained.	<i>PLINIAN PUMICE FALL</i> : widely dispersed thin topography-mantling sheets of well-sorted stratified pumice derived from high eruption columns (Fisher and Schminke, 1984; Houghton et al., 2000a). <i>REWORKED PLINIAN FALL</i> : scoured bases, lenticularity, cross lamination, loss of delicate vitric components & introduction of lithics indicate remobilization by water. <i>PHREATOPLINIAN FALL</i> : exceptionally fine grain size, shard morphologies and sedimentary structures indicate interaction of vesiculating magma with surface water producing abundant steam and very fine, water-saturated cohesive ash (Self and Sparks, 1978; Self, 1983; Heiken and Wohletz, 1985; Cioni et al., 1992; McPhie et al., 1993; Wilson et al., 1995; Morissey et al., 2000; Houghton et al., 2000b).	<i>PLINIAN PUMICE FALL</i> : Sharp bedding planes imply a spasmodic, nonsustained eruption column (Houghton et al., 2000a) possibly indicating subplinian rather than plinian eruptive style (Cioni et al., 2000). <i>REWORKED PLINIAN FALL</i> : Similar to deposits in the Rotongaio ash (New Zealand), interpreted to record short but regionally extensive rain shower events (Smith and Houghton, 1995). <i>PHREATOPLINIAN FALL</i> : Lack of accretionary lapilli may be an artifact of preservation, or may indicate very wet conditions (Jurado-Chichay and Walker, 2001). General lack of nonjuvenile rock fragments may indicate interaction with water at shallow levels in the conduit, i.e., with surface water rather than aquifers (Allen and Cas, 1998; De Rita et al., 2002).

basinal granites, to a variety of pyroclastic matrix types, reflecting remobilization of freshly-erupted debris on talus cones and debris-flow fans. We subdivide the boulder breccia-conglomerates into the following types of deposits, with increasing distance from the Sawmill Canyon fault zone over a distance of 8.5 km: talus deposits, proximal debris-flow deposits, medial to distal debris-flow deposits, and minor stream-flow deposits (Table 1; *ESM*).

#### Dacitic block-and-ash-flow tuffs

The dacitic block-and-ash-flow tuffs (Fig. 4) are interpreted as small-volume pyroclastic flows generated by gravitational dome collapse (e.g. Fisher et al. 1980; Sparks 1997; Freundt et al. 2000). The coarse grain size and (rare) occurrence of amoeboid clasts suggest that the collapsing dome or domes lay nearby, yet the lack of vent facies (dacitic intrusions or lava flows/domes) within the basin indicates that the domes were extrabasinal. The dramatic decrease in grain size away from the Sawmill Canyon fault zone indicates that the source domes lay along the fault, or just across the fault zone from the basin. We infer that the domes were plumbed up through the fault zone, and then tectonically dismembered along it, because the vent facies does not appear to be preserved.

#### Andesitic lava flows, flow breccias and intrusions

The andesitic lava flows are largely brecciated units, with coherent interiors, that do not crosscut stratigraphy, and have void spaces between vesicular blocks infilled by

overlying tuffs or sediments. They commonly show flow banding and flow aligned crystals.

The andesitic intrusions are largely coherent (nonbrecciated), generally nonvesiculated units that, at least locally, cross-cut stratigraphy and generally have a higher crystal content than the lava flows. The thicknesses of the intrusions, their limited lateral extent, and the alternation of sills with brecciated lava suggest emplacement as sill-like bodies that intruded early-erupted flows and vented locally to feed more lava flows (Fisher and Schminke 1984; Fink and Anderson 2000). These vents are sited on syndepositional faults (Fig. 2).

#### Andesitic vulcanian breccia

Clast-supported andesitic breccias form a 500 m thick sequence in the master fault-proximal sub-basin (Fig. 2). We interpret these breccias as the proximal deposits of vulcanian explosions. The great thickness, uniformly coarse grain size, and crude stratification suggests that the vent lay close by, probably along the Sawmill Canyon fault zone (but now dismembered), and that the vulcanian breccia was ponded within the basin.

#### Andesitic ignimbrites, vitric tuffs, and tuffaceous sandstones

The andesitic ignimbrites are massive, poorly sorted, crystal-rich tuffs with abundant flattened scoria, bubble-wall shards (rarely welded), and lesser cognate lithic fragments. They are



interbedded with andesitic lava flows (Fig. 2). Three of the four andesitic ignimbrites occur at the bases of andesitic lava flow or vulcanian breccia sequences (Figs. 2, ESM); these may therefore represent the first, degassing phase of the andesitic eruptions (Fisher and Schmincke 1984).

The andesitic vitric tuff and tuffaceous sandstones (Fig. 5a) have much the same componentry as the andesitic ignimbrites, except for the presence of blocky and splintery shards in addition to bubble-wall shards, indicating phreatomagmatic as well as magmatic fragmentation mechanism (Fig. 5b, c, Table 1). In outcrop, their sedimentary structures indicate fluvial reworking by hyperconcentrated flood flow, with high sedimentation rates.

Rhyolitic intrusions, lava domes—dome breccias, block-and-ash-flow tuffs

Rhyolitic intrusions occur as massive basal sills and plugs that pass upward and laterally into rhyolitic lava domes and dome breccias. The intrusions have irregular contacts and crosscut lithofacies contacts within the basin. They are commonly offset by faults at their bases with decreasing offset upsection, indicating that vent locations were fault controlled. We interpret the rhyolitic intrusions as shallow level intrusions that supplied magma to intrabasinal domes upsection.

Lava domes are composed of flow-banded coherent rhyolite mantled by or interbedded with dome breccia. The lava domes are sited on intrabasinal faults, which acted as conduits for the plugs described above (Fig. 2). The rhyolitic lava domes are small and bulbous, and are interpreted to be the result of endogenic dome growth. The blocks in the lava domes are relatively small (1–2 m maximum diameter) suggesting relatively high extrusion rates (Fink and Anderson 2000).

The rhyolitic dome–dome breccias are fringed by rhyolitic block-and-ash-flow tuffs, interpreted to represent pyroclastic flows generated by lava dome collapse.

Rhyolitic ignimbrites

The rhyolitic, crystal-poor ignimbrites are interstratified with rhyolitic domes and plinian to phreatoplinian tuffs in the northern sub-basin (Fig. 2). Weakly erosive basal contacts suggest a vent proximal deposit (Freundt et al. 2000). Blocky shards indicate a phreatoplinian eruptive style, in addition to cusped shards typical of plinian eruptive styles (Heiken and Wohletz 1985; McPhie et al. 1993; De Rita et al. 2002). The presence of local cross-stratification and sorting suggests minor fluvial reworking.

The rhyolitic, white, high-grade ignimbrite consists largely of moderately-welded pumice lapilli tuff, with well-preserved vitroclastic textures, but it contains several banded horizons interpreted to be ultrawelded ignimbrite (Figs. 2, ESM). The

ultrawelded banded horizons show extremely attenuated fiamme, sintering, plastic deformation of shards, and planar to contorted flow banding. These features are commonly attributed to primary deformation of high-temperature pyroclastic flows during transport and deposition (Branney and Kokelaar 1992; McCurry et al. 1996; Freundt 1999) or secondary rheomorphic flowage after deposition and deflation (Schmincke and Swanson 1967; Wolff and Wright 1981). The alternation of ultrawelded with weakly welded horizons indicates multiple cooling units, suggesting either fluctuation in the eruptive column or multiple ignimbrite emplacement. The absence of blocky shards, and the high emplacement temperatures required for strong welding, indicates that the eruption was “dry” (i.e. no interaction with surface water). Like the rhyolitic, crystal-poor ignimbrites, the rhyolitic, white, high-grade ignimbrite lies in the master fault-proximal (northern) sub-basin, unlike all the other rhyolitic ignimbrites, which lie largely or entirely within the master fault-distal (southern) sub-basin.

The rhyolitic crystal-rich ignimbrites occur as two white, nonwelded pumice lapilli tuffs, each 5–20 m thick (Figs. 2; ESM). They are the most crystal-rich silicic ignimbrites in the Santa Rita Glance Conglomerate, with 30–35% large quartz and biotite phenocrysts (3–4 mm).

The rhyolitic lithic-rich ignimbrite (Fig. 2) has ~20–30% angular lithic fragments, ranging in size from 5 cm to 2 m in diameter, and is crystal poor (<15%), with abundant nonwelded bubble-wall shards. It varies in thickness from ~10 m near the central structural high to >50 m in the southern sub-basin.

The rhyolitic limestone-lithic ignimbrite (Fig. 2) has limestone clasts in the nonwelded horizons, and these clasts show variable degrees of metamorphism to marble and amphibolite that correspond to density of welding in the welded horizons, indicating that the clasts were metamorphosed in situ. This ignimbrite reaches >60 m in total thickness, and consists of four cooling units, with the basal cooling unit thickest at ~30 m; it occurs at a single stratigraphic horizon in the master fault-distal (southern) sub-basin only (Figs. 2 and ESM). The rhyolitic limestone-lithic ignimbrite is the only ignimbrite that contains limestone clasts.

The rhyolitic, red, high-grade ignimbrites are ultrawelded, crystal-poor, pumice lapilli tuffs only a few meters thick that serve as distinctive stratigraphic marker horizons across the fault-proximal and fault-distal sub-basins (Figs. 2 and ESM). They are predominantly ultra-welded with fiamme showing strong eutaxitic foliation, although the upper ignimbrite is only moderately welded in the southern sub-basin. The top contacts and thinner deposits are brecciated and/or spherulitic. The breccias resemble auto-breccias of lava flows, but they pass laterally and irregularly into undisturbed, flat-lying eutaxitic ignimbrite, and the outlines of the blocks are commonly faint. Hot-state



**Fig. 3** Proximal debris-flow deposit (boulder breccia-conglomerate lithofacies), with angular blocks to pebbles of a wide variety of clast types, supported in a brick-red matrix of granitic granules and coarse-grained arkosic sandstone

brecciation likely occurred during rheomorphic flow in the late stages of cooling, a common feature of high-grade “lava-like” ignimbrites (Branney and Kokelaar 1992, 1994; Beddoe-Stephens and Millward 2000). The upper of the two rhyolitic, red, high-grade ignimbrites can be mapped continuously for ~7 km and then traced for another ~4.5 km as a single layer of 2–3 m blocks within boulder breccia-conglomerates of the fault-proximal sub-basin.

#### Rhyolitic plinian and phreatoplinian tuffs

Laterally continuous, thin-bedded rhyolitic tuffs and pumice lapillistones (Fig. 6) occur throughout much of the basin fill (Fig. 2). These include: (1) plinian pumice fall deposits, (2) reworked plinian pumice fall deposits, and (3) phreatoplinian ash fall deposits.

Alternations of plinian and phreatoplinian tuffs may result from (1) phreatomagmatic fragmentation reverting to magmatic fragmentation when the water supply is exhausted, as discussed by Self (1983); (2) a switch from magmatic to

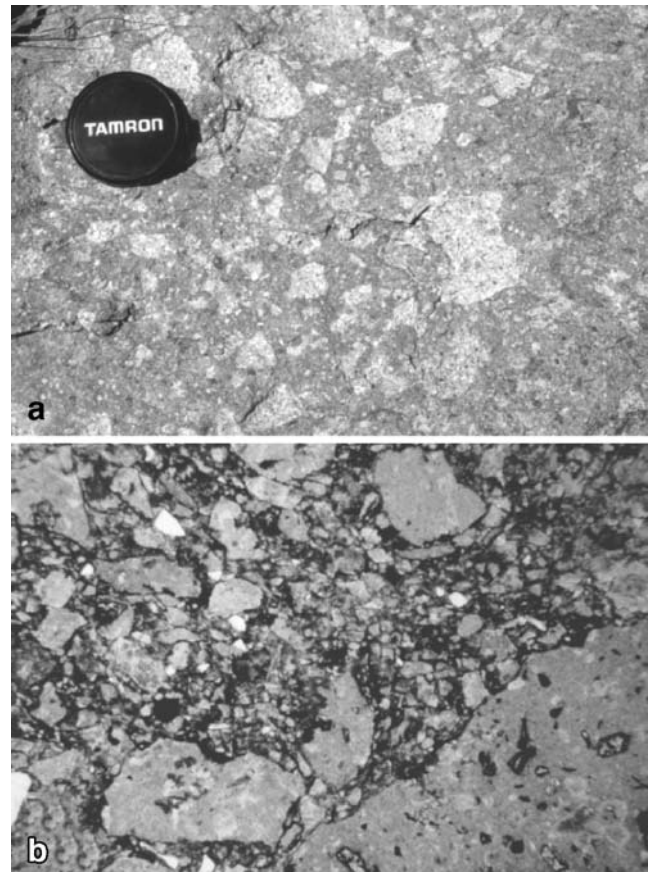


**Fig. 4** **a** Outcrop photo of dacitic block-and-ash-flow tuff, showing nonvesiculated (dense) angular clasts, all of the same crystal-poor dacite, supported in an unsorted, coarse ash matrix of the same composition (lens cap for scale). **b** Photomicrograph of ash-sized matrix of a dacite block-and-ash flow tuff, consisting of the same dense (nonvesiculated), angular, unsorted clasts as the larger lapilli and blocks visible in outcrop (field of view=8 mm)

phreatomagmatic eruption style, reflecting a reduction of magma flux that somehow allowed water to enter the vent (Jurado-Chichay and Walker 2001); or (3) nonsystematic alternations, perhaps resulting from variability in water influx to the vent (Self 1983; Wohletz 1986; Jurado-Chichay and Walker 2001). The plinian and phreatoplinian tuffs (Table 1) form very thick sections, some many tens of meters thick containing rock fragments and large crystals, suggesting that they are vent-proximal accumulations.

#### Spatial distribution of lithofacies

The spatial distribution of volcanic lithofacies and vents (Fig. 2) is controlled by the structure of the basin, which is inferred to be a releasing-bend strike-slip basin (Figs. 7 and 8, discussed further below). This spatial distribution is shown in simplified form in Fig. 9.

Rhyolitic domes, dome breccias and intrusions are restricted to intrabasin faults in the northern sub-basin,

proximal to the Sawmill Canyon fault zone (Figs. 2 and 9). The rhyolitic dome–dome breccia lithofacies is fringed by the rhyolitic block-and-ash-flow tuff lithofacies, and is interbedded with rhyolitic, white, crystal-poor ignimbrites or rhyolitic plinian-phreatoplinian tuffs (Figs. 2, *ESM* and Table 1). This records alternating effusive and explosive silicic volcanism within the basin, through vents controlled by syn-depositional faulting. We infer that the rhyolitic, white high-grade ignimbrite was erupted from an intrabasin vent because it has the same white color and low crystal content as the rhyolitic intrusions, domes and dome breccias, block-and-ash-flow tuffs and crystal-poor ignimbrites. The rhyolitic, white high-grade ignimbrite is restricted to a single stratigraphic horizon within a section of rhyolitic crystal-poor ignimbrites that are nonwelded with blocky shard, suggesting that water gained access to intrabasin ignimbrite vents much more commonly than not.

The association of andesitic intrusions with thick successions of andesitic lava flows and vulcanian breccias indicates intrabasin venting (Figs. 2, *ESM*, 9 and Table 1). Andesitic intrusions and lava flows occur along faults in both sub-basins. Reworked andesitic vitric tuffs accumulated to great thickness in the fault-distal sub-basin (Figs. 2 and 9b), probably because the fault-proximal sub-basin was

kept too full of vent-proximal volcanic rocks and conglomerate-breccia to accommodate reworked tuffs (Fig. 9c).

We infer that some lithofacies in the Santa Rita Glance Conglomerate had sources, now dismembered, along the Sawmill Canyon fault zone. These include (Figs. 2 and 9 and Table 1): (1) the boulder breccia-conglomerates, (2) the dacitic block-and-ash-flow tuffs, and (3) the andesitic vulcanian breccia.

Four types of rhyolitic ignimbrite are interpreted as extrabasally sourced (Fig. 9b) because they differ from the intrabasin ignimbrites in phenocryst and lithic compositions (Table 1), and because the very well-exposed basin fill contains no candidates for vents or vent-proximal deposits with similar mineralogy, such as intrusions, ignimbrite feeder dikes (*sensu* Aguirre-Diaz and Labarthe-Hernandez 2003), proximal ejecta lobes or rings (*sensu* Fierstein et al. 1997), or co-ignimbrite lag breccias (*sensu* Druitt and Sparks 1981). In addition, one ignimbrite has limestone lithics, and there is no limestone in the substrate or margins of this basin, although limestones occur in other ranges along and northeast of the Sawmill Canyon fault zone (Fig. 1). They are thus accidentally ponded ignimbrites, with thicknesses that nowhere rival typical caldera fill. The extrabasally-sourced rhyolitic ignimbrites occur

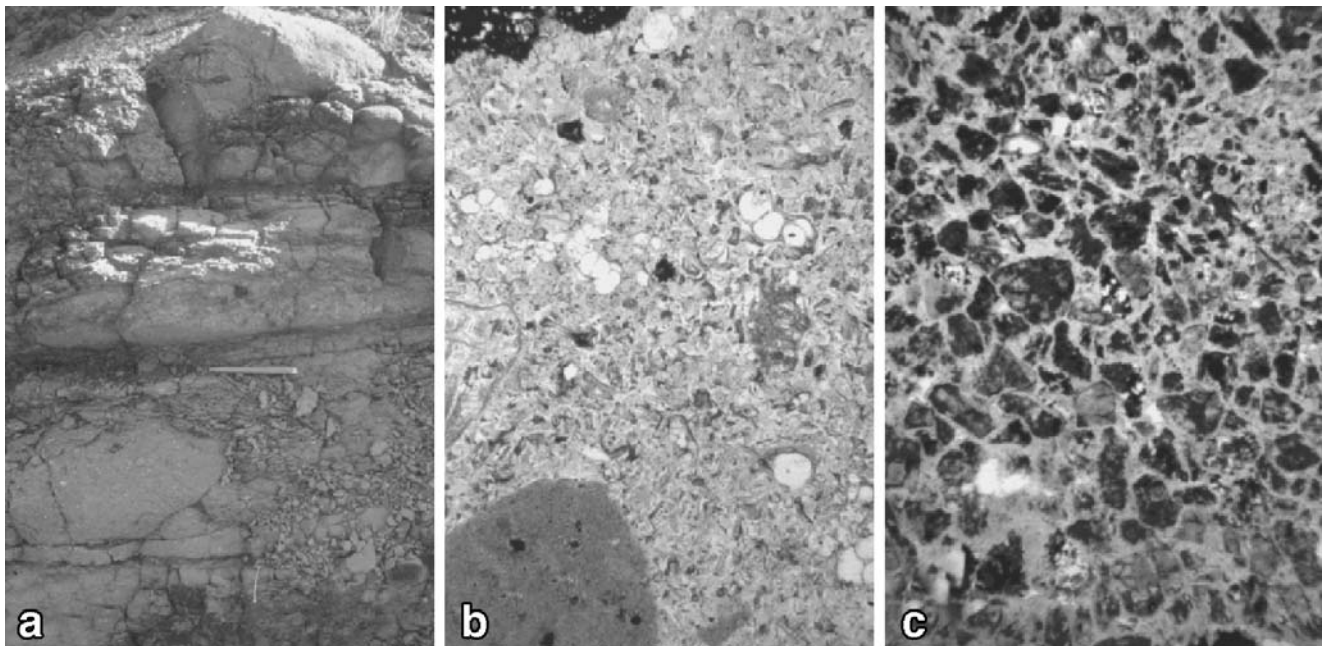


**Fig. 5** **a** Outcrop photo of the andesitic vitric tuff and tuffaceous sandstone lithofacies (pencil for scale). These deposits are bedded, laminated and cross-laminated, with cut and fill structures, causing some workers to call them sandstones (see Drewes 1971), but in thin section, most samples are composed entirely of pyroclastic debris. **b** Photomicrograph of a tuffaceous volcanic lithic sandstone from the andesitic vitric tuff and tuffaceous sandstone lithofacies (field of view=6 mm). This sample was taken from a cross-laminated bed that shows clear evidence of fluvial reworking. Two different types of andesitic

volcanic rock fragments (*top left and bottom left*) and a plagioclase crystal (*center left*) lie in a matrix of scoria fragments and bubble-wall shards. The preservation of delicate bubble-wall shards and scoria fragments indicates minimal fluvial reworking of freshly-erupted pyroclastic debris. **c** Photomicrograph of a vitric tuff from the andesitic vitric tuff and tuffaceous sandstone lithofacies (field of view=6 mm). In contrast with the sample shown in **b**, this sample is composed of blocky to splintery shards inferred to have formed by explosive interaction of magma with ambient water (groundwater or lakes)



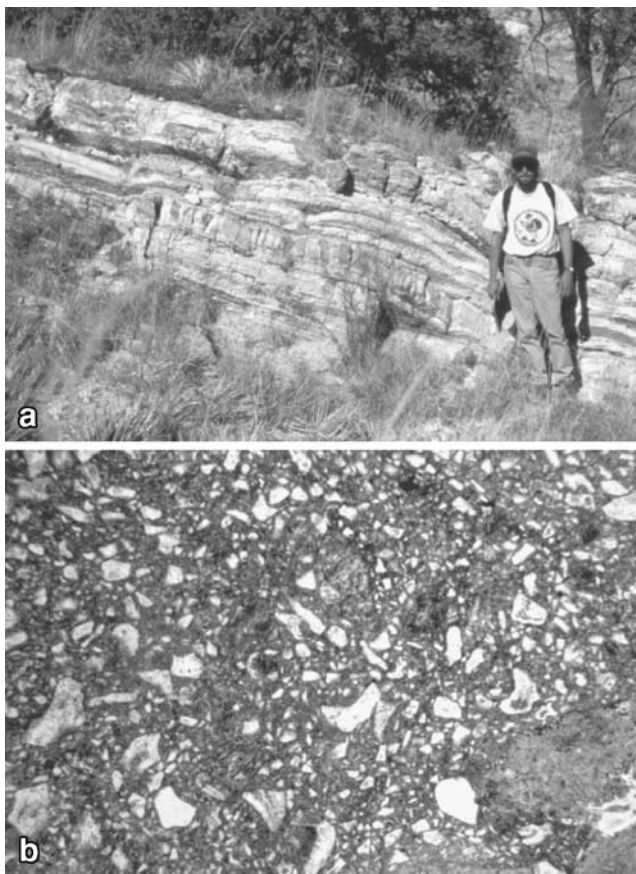


**Fig. 6** **a** Outcrop photo of the rhyolitic plinian and phreatoplinian tuff lithofacies. These form widespread sheets only a few meters thick that mantle topography. **b** Photomicrograph of a rhyolitic phreatoplinian tuff (field of view=6 mm). This sample consists of blocky to splintered glass shards, set in an optically irresolvable fine-grained matrix. These are interpreted as phreatoplinian ash fall deposits, which record explosive eruptions through water

largely in the fault-distal sub-basin but some spill over the central structural high for a short distance into the fault-proximal sub-basin (Figs. 2 and 9b; Table 1). Each of these ignimbrite types is restricted to one or two stratigraphic levels; this fact, and their distinctive textures and compositions, make them useful marker horizons that help correlate the sequences of the fault-proximal and fault-distal sub-basins (Bassett and Busby 2005). The extrabasally-sourced ignimbrites were preferentially ponded in the master fault-distal (southern) sub-basin even though it subsided less than the fault-proximal sub-basin, because fault-proximal sub-basin was kept full by intrabasinal volcanism and sediments shed from the master fault (Fig. 9c).

### Syndepositional faults

The structural evolution of the basin is described in detail by Bassett and Busby (2005), and summarized briefly here.

The regionally significant Sawmill Canyon fault zone (Fig. 2) is inferred to be the dominant basin-bounding fault because boulder clast size and angularity increase toward it, the boulder breccia-conglomerate lithofacies becomes more proximal toward it, the basin fill generally thickens toward it, and intra-basinal, syndepositional faults show the greatest displacement near it. Reactivation of the Sawmill Canyon fault zone during the Late Cretaceous to Early Tertiary Laramide Orogeny juxtaposed younger and older units against the Santa Rita Glance Conglomerate.

A less regionally significant fault zone, the Gringo Gulch fault zone, bounds the south end of the basin (Fig. 2). This fault cuts the Santa Rita Glance Conglomerate and its basement (Jurassic Squaw Gulch granite, Fig. 2) and it is cut by the Late Cretaceous Josephine Canyon diorite (Drewes 1971). This subvertical fault is en echelon to the Sawmill Canyon fault zone. Andesitic flows and sills are abundant at the south end of the basin (Figs. 2 and 9b), suggesting that the Gringo Gulch fault plumbed magmas to the surface (Fig. 9c).

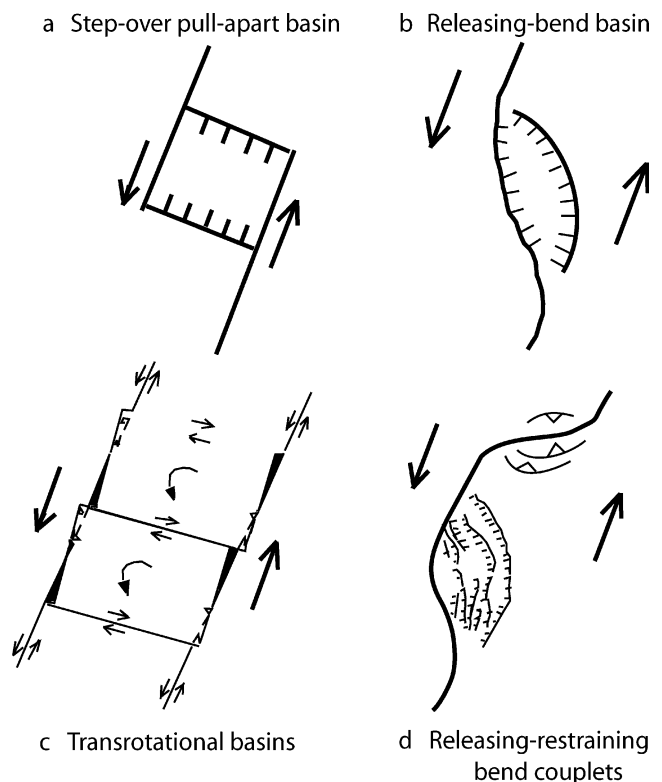


**Fig. 7** Three major types of strike-slip basins (after Nilsen and Sylvester 1995), including **a** pull-apart basin, **b** releasing bend basin, and **c** transrotational basins. Also shown is **d** releasing- and restraining-bend couplet along an overall transtensional strike-slip fault, where the restraining bend is smaller than the releasing bend (after Cowan et al. 1989; Cowan and Pettinga 1992); bends are exaggerated to display geometries clearly, whereas in nature, very subtle bends produce similar structures



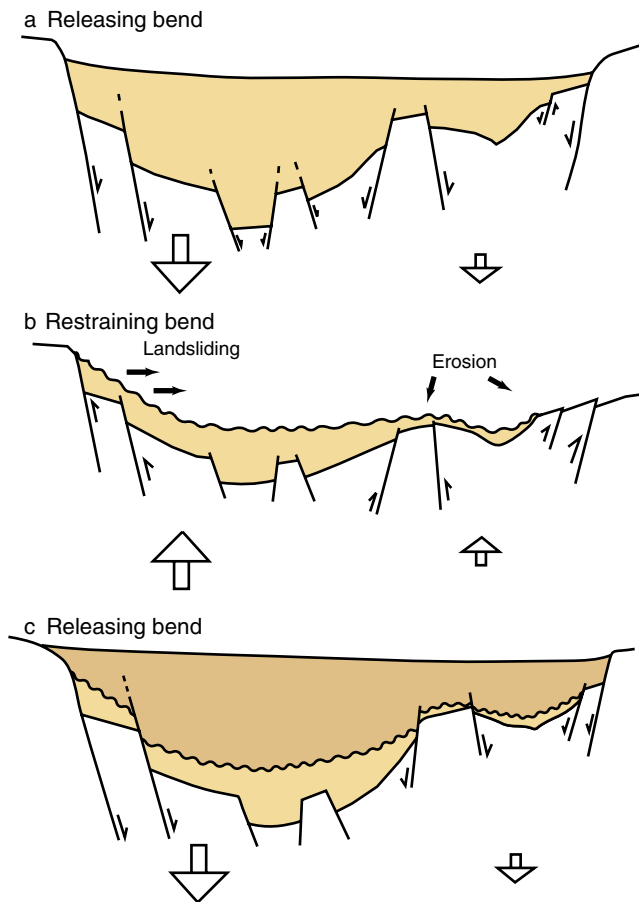


**Fig. 8** Cartoon cross section illustrating “porpoising” of a strike-slip basin as it slides past alternating releasing and restraining bends of a strike-slip fault. The “deep” end of the basin (*left*) is bounded by the major strike-slip fault. **a** Normal faulting and subsidence at a restraining bend, accommodating accumulation of a thick stratigraphic sequence; **b** Reverse faulting and uplift at a restraining bend causes erosion of basin fill, creating deep unconformities; **c** Renewed normal faulting and subsidence along a releasing bend. This may repeat several times. An overall transtensional fault is shown, where net subsidence over time will result in partial preservation of a basin fill that is divided by deep unconformities

The basin also contains numerous intrabasinal syndepositional high-angle faults (Figs. 2 and 9) that alternated between normal-slip and reverse-slip separation. At some times, faults with normal separation were active synchronously with faults showing reverse separation elsewhere in the basin (Bassett and Busby 2005). Intrabasinal faults subdivide the basin into master fault-proximal (northern) and fault-distal (southern) sub-basins, separated by a structural high (Figs. 2 and 9). The master fault (Sawmill Canyon fault zone) served as the primary conduit for andesitic to rhyolitic magmas; however, the smaller faults also served as conduits for smaller volumes of magma and controlled intrabasinal vent sites.

## Unconformities

Eight large-scale deep unconformities cut the basin fill (shown in blue on Fig. 2), dividing it into eight unconformity-bounded sequences (Bassett and Busby 2005). These unconformities are easily mapped out because they incise deeply into underlying strata (Figs. 2 and 9b, c). Five of the eight unconformities show extreme vertical relief (460–910 m) and very high paleo-slope gradients (40°–71°); they lie in the master fault-proximal (northern) sub-basin where they face asymmetrically away from the master fault (Figs. 1 and 9b, c). These are interpreted to represent fault scarps and paleo-slide scars produced during basin uplift (“basin inversion”) events at restraining bends along the master fault (Bassett and Busby 2005). Unconformities in the master fault-distal (southern) sub-basin, in contrast, are symmetrical, with vertical relief of 200–600 m and paleo-slope gradients of 20°–25° (Figs. 1 and 8b, c). These are interpreted to represent deep paleocanyons (Bassett and Busby 2005).

## Volcanic facies model for the Santa Rita Glance intra-arc strike-slip basin

All previously-published facies models for strike-slip basins were developed for siliciclastic systems; we present the first facies model for an intra-arc strike-slip basin (Fig. 9c). This volcanic facies model may be applicable to releasing-and-restraining-bend basins that form along curves in strike-slip faults within arcs. The name “releasing-restraining bend intra-arc strike-slip basin” emphasizes the fact that transtensional and lesser transpressional processes, as well as magmatic processes, mold the basin and its volcanic fill as it slips along the strike-slip fault. The unconformities and syn-depositional faults are at least as important as the volcanism for controlling the architecture of the basin fill. Thus, our basin model has two distinguishing characteristics: the unconformities, which are created at restraining bends, and the small, numerous polygenetic volcanic complexes, which form at releasing bends of an intra-arc strike-slip fault zone.

Strike-slip basins largely occur as three major types (Nilsen and Sylvester 1995): (1) classical pull-apart basins, which form at a releasing stepover between *en echelon* segments of a strike-slip fault (Fig. 7a), (2) releasing bend basins, which form along a gently curved strike-slip fault (Fig. 7b), and (3) transrotational basins, which form at the trailing edge of a crustal block under vertical axis rotation (Fig. 7c). Pull-apart basins are symmetrical and subside continuously along normal-slip separation faults (Fig. 7a). Transrotational basins are asymmetrical, wedge-shaped basins that subside along normal-slip separation faults

**Fig. 9** Volcanological facies architectural model for an intra-arc strike slip basin: **a** Map view of the inferred structural setting, modeled after the modern Glynn Wye Basin along the Hope Fault, New Zealand (after Cowan et al. 1989 and Cowan and Pettinga 1992; for details see Bassett and Busby 2005). **b** Down-dip view of the basin based on the outcrop lithofacies map (Fig. 2), with colors keyed to it. The inferred structural setting of line of this down-dip view is shown on Fig. 9a. **c** Interpretive block diagram showing volcanic facies architecture (*front of block*) and inferred processes (*top of block*) in an intra-arc strike slip basin, based on the Santa Rita Glance Conglomerate. This model is broadly applicable to releasing- and restraining-bend intra-arc basins, which form at curves in the traces of strike slip faults. Colors are keyed to the lithofacies map (Fig. 2) and the down-dip view of the basin (Fig. 9b); the front of the block is shown in somewhat bolder colors than the top of the block

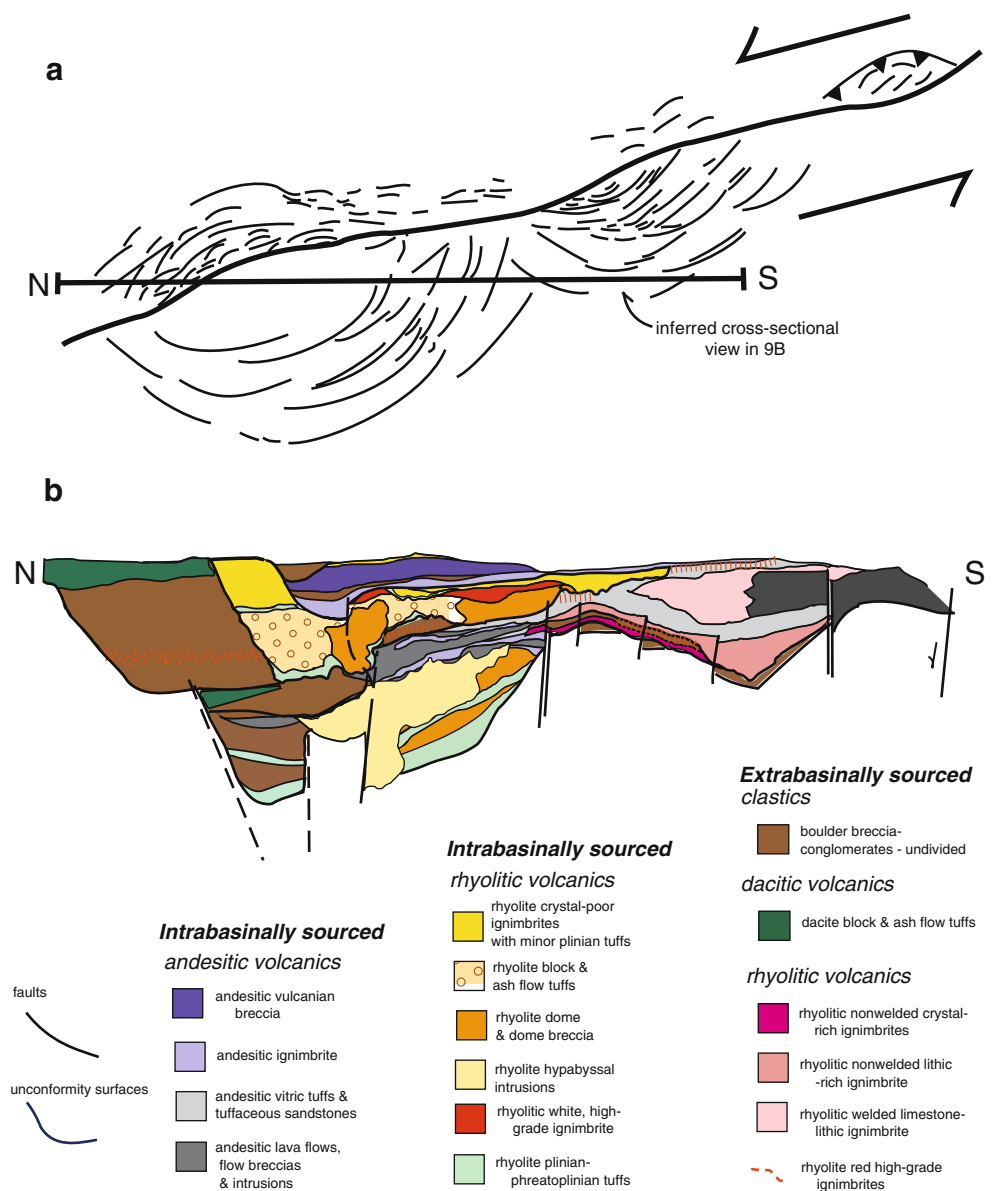
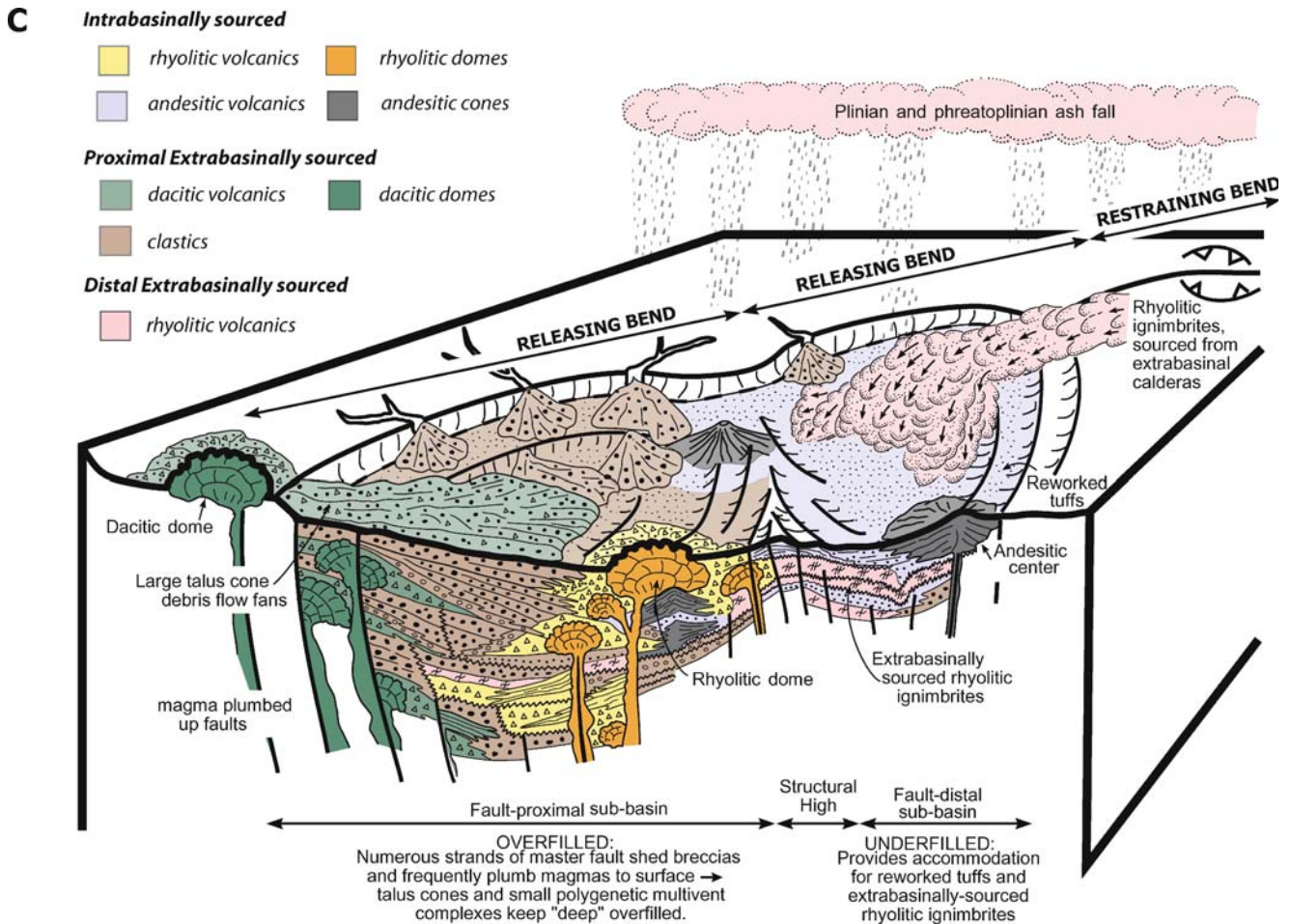


(Fig. 7c). Releasing bend basins are also asymmetrical (Fig. 7b), but the broad curves that produce releasing bends along strike-slip faults also tend to produce restraining bends, resulting in alternating releasing and restraining bends along the length of the fault (Fig. 7d). This results in “porpoising,” or alternating subsidence and uplift of the basin as it slips along the fault, as first described by Crowell (1974). This “porpoising,” and its effects on the basin architecture, are illustrated in Fig. 8.

The structural style of strike-slip faults with releasing-restraining bend couplets consists of a major basin-bounding strike-slip fault and smaller intra-basinal faults (Figs. 7d, 8 and 9a). These faults show reverse and normal components of slip that develop simultaneously with grabens and arches, in positions that vary rapidly through time (Crowell 1982; Christie-Blick and Biddle

1985; Wood et al. 1994; Nilsen and Sylvester 1995; Barnes and Audru 1999; Barnes et al. 2001). The dip on the master strike-slip fault controls the width of the releasing-bend basin. Where there is a close spatial and temporal association of releasing and restraining bends, basin subsidence alternates with basin uplift on a time scale of  $10^5$  to  $10^6$  years, producing large-scale intrabasinal unconformities (Fig. 8; Wood et al. 1994; Barnes et al. 2001). If the restraining bends are of the same scale as the releasing bends, all of the basin fill created at a releasing bend should be inverted and eroded away at the succeeding restraining bend. When a strike-slip fault system is overall slightly transtensional, however, the restraining bends are smaller than the releasing bends (Figs. 7d and 9a), and net subsidence over time will result in partial preservation of the basin fill (Fig. 8). We refer to

Fig. 9 (continued)



this type of basin as a ‘releasing- and restraining-bend basin’ to emphasize the fact that very deep unconformities are an important feature of the basin fill (Fig. 8).

Numerous, very deep unconformities bound volcanic and sedimentary sequences in the Santa Rita Glance Formation (Fig. 9b). Each of these very deep unconformities was produced by partial basin inversion (uplift) along a restraining bend, followed by deep burial due to subsidence at the next releasing bend (Fig. 8); these processes alternated as the basin slipped along the strike-slip fault. The restraining bends must have been smaller than the releasing bends (Fig. 7d), because net subsidence over time resulted in partial preservation of the basin fill.

Volcanic and subvolcanic rocks in the strike-slip basin formed multiple small, polygenetic vent complexes in a complexly-faulted basin (Figs. 2 and 9b). We thus interpret the volcanic rocks of the Santa Rita Glance Conglomerate to be a rhyolitic to dacitic to andesitic multivent, polygenetic complex with hypabyssal intrusions that map directly into effusive and explosive volcanic deposits (Fig. 9c).

There is no evidence that the basin represents one or more calderas, because there are no very thick silicic ignimbrites typical of caldera fill; ring faults and ring fracture intrusions are absent, nor are there any of the slide sheets typically formed by caldera collapse. Instead, the intrabasally-sourced lithofacies of the Santa Rita Glance Conglomerate record repeated intrabasinal intrusion and venting of relatively small volumes of magma along intrabasinal faults, with subequal intermediate and silicic compositions, and subequal effusive and explosive eruptive styles. Interfingering of eruptive products indicates that more than one vent was active at a time, hence the name “multivent complex” is applied. We propose that multi-vent complexes reflect proximity to a continuously active fault zone, where strands of the fault frequently plumb small batches of magma to the surface at releasing bends. Intrabasinal faults ponded ignimbrites and locally plumbed magma to the surface (Fig. 9c).

Dacitic domes that lay just outside the basin to the north produced proximal block-and-ash-flow tuff breccias that fine with distance from the master fault (Fig. 9c); they are

interbedded with the boulder breccia-conglomerates in the fault-proximal sub-basin, and supplied sand-sized material (ash) for the breccia-conglomerate matrix. These dacite domes were probably plumbed up the master fault (Fig. 9c), just as modern dome chains are commonly sited on faults (Bailey 1989; Bellier and Sebrier 1994; Bellier et al. 1999).

Andesitic magmas inflated the section as sills, and locally vented out onto the surface as lava flows and lesser ignimbrites (Figs. 2 and 9). Andesitic tuffs also contain shard morphologies typical of phreatomagmatic eruptions, and were commonly reworked by fluvial processes, suggesting a wet climate (Busby et al. 2005).

Growth of intrabasinal rhyolitic lava domes (Figs. 2 and 9c) produced both block-and-ash-flow tuff breccias and dome breccias, depending on the temperature of the parental lava during disintegration into avalanches. Highly vesiculated silicic magma produced plinian eruptions, forming plinian ashfall and pumiceous pyroclastic flow deposits. Plinian eruptions through surface water resulted in phreatoplinian eruptions, which, together with fluvially-reworked tuffs, suggest a wet climate. The pumiceous pyroclastic flow deposits (ignimbrites) are generally non-welded and contain blocky shards in addition to bubble-wall shards, again suggesting a dominantly “wet” eruptive style (Busby et al. 2005).

Most of the ignimbrites in the Santa Rita Glance Conglomerate are inferred to be extrabasinally-sourced, because their mineralogy is distinct from volcanic rocks that can be traced directly into intrusions within the basin. Their sources are most likely from calderas located at releasing step-overs elsewhere along the Sawmill Canyon strike-slip fault zone (Busby et al. 2005).

Intrabasinal normal- and reverse-slip separation faults controlled the positions of local arches and grabens (Fig. 9c), leading to abrupt thinning and thickening of strata and local intrabasinal venting, but the basin fill broadly thins away from the master fault (Sawmill Canyon fault zone) toward the subordinate basin-bounding fault (Gringo Gulch fault zone). Talus cone-alluvial fan deposits are restricted to the deep end of the basin (Fig. 9c). Most of the proximal extrabasinal volcanic rocks were erupted from the master fault zone and trapped in the deep end of the basin. Most of the intrabasinal volcanic rocks were erupted from intrabasinal faults in the deep (master fault-proximal) end of the basin (Fig. 9). This volcanism, in combination with master-fault proximal clastic sedimentation, kept the deep end of the basin completely full. In contrast, the master-fault distal sub-basin was able to accommodate extrabasinally-sourced ignimbrites and fluvially reworked pyroclastic deposits (Fig. 9c).

The closest modern analogue to the Santa Rita Glance Conglomerate is probably the Sumatra volcanic arc in Indonesia, a continental transpressional to transtensional

arc. Small volcanic centers (in Sumatra, mainly rhyolite domes) occur along releasing bends (e.g. Fig. 7c), whereas caldera complexes occur along releasing step-overs, in pull-apart basins (e.g. Fig. 7a; Bellier and Sebrier 1994; Chesner 1998; Bellier et al. 1999; Ventura 1994). In the Late Jurassic arc of southern Arizona, small, multivert, polygenetic eruptive centers formed along releasing bends in the strike-slip fault (Santa Rita Glance Conglomerate), but the deposits of these interfinger with ignimbrite outflow sheets erupted from calderas at releasing stepovers along the Sawmill Canyon fault zone (Busby et al. 2005).

## Conclusions

The Late Jurassic basin described in this paper affords a time-integrated view of an intra-arc strike-slip basin that workers in modern arcs do not have. Strands of the Sawmill Canyon strike-slip fault zone both bounded and lay within the releasing-and restraining-bend basin. These plumbed small batches of silicic and intermediate-composition magma to the surface, resulting in frequent, small-volume, polygenetic (explosive and effusive) eruptions from multiple vents within and along the margins of the complexly faulted basin. When the basin slipped through small restraining bends in the strike-slip fault, it was uplifted, and deep unconformities were carved into the basin fill; when the basin slipped through releasing bends, rapid subsidence occurred, providing preservation space for the arc volcanic rocks. The basin fill thinned and intrabasinal volcanism decreased dramatically away from the master strike-slip fault, where subsidence was greatest and fault-controlled vents most abundant. Talus cones and alluvial fan deposits were largely restricted to the “deep” end of the basin (next to the master strike-slip fault), and lava domes sited on the master fault shed block-and-ash flows into the “deep” end of the basin. The master-fault-proximal end of the basin was thus “overfilled,” while the “underfilled” master-fault-distal end of the basin provided accommodation for reworked tuffs, as well as extrabasinally-sourced ignimbrites. These accidentally-ponded ignimbrites were erupted from calderas at releasing step-overs elsewhere along the Sawmill Canyon fault zone (Busby et al. 2005); large-volume ignimbrite eruptions and caldera collapse did not occur in the releasing-and restraining-bend basin.

The three-dimensional arrangement of deposits in intra-arc strike-slip basins is controlled not only by volcanic processes, but also by tectonic processes, including structural controls on patterns of uplift and subsidence, on locations of vents, and on types of centers that develop.

**Acknowledgements** We gratefully acknowledge formal reviews by Rick Conrey, Julie Donnelly-Nolan, Nancy Riggs and the late, truly extraordinary Tor Nilsen. We are indebted to Nancy Riggs, Bill



Dickinson, Peter Lipman, Ken Hon, Gordon Haxel, Peter Kokelaar, and CB's mentor, the late marvelous Richard Fisher, for discussions in the field in southern Arizona. Discussions with Jarg Pettinga, John Crowell and Rebecca Dorsey are also gratefully acknowledged. Robert Bothmann and Senta provided invaluable field assistance. CB would like to acknowledge her three daughters, Claire, Sophia, and Marion, for accompanying her on day-long, cross-country traverses over very rugged terrane at ages as young as four years. Support was provided by NSF-EAR 92-19739 awarded to Busby.

## References

- Aguirre-Diaz GJ, Labarthe-Hernandez G (2003) Fissure ignimbrites: fissure-source origin for voluminous ignimbrites of the Sierra Madre Occidental and its relationship with Basin and Range faulting. *Geology* 31:773–776
- Allen PA (1997) Earth surface processes. Blackwell Science, Oxford
- Allen SR, Cas RAF (1998) Rhyolitic fallout and pyroclastic density currents from a phreatoplinian eruption in the eastern Aegean Sea, Greece. *J Volcanol Geotherm Res* 86:219–251
- Bailey RA (1989) Quaternary volcanism of Long Valley caldera, and Mono-Inyo Craters, Eastern California: 28th International Geological Congress, Field trip Guidebook T313, American Geophysical Union, Washington, DC
- Barnes PM, Audru J-C (1999) Recognition of active strike-slip faulting from high-resolution marine seismic reflection profiles: Eastern Marlborough fault system, New Zealand. *Geol Soc Am Bull* 111:538–559
- Barnes PM, Sutherland R, Davy B, Delteil J (2001) Rapid creation and destruction of sedimentary basins on mature strike-slip faults: an example from the offshore Alpine Fault, New Zealand: *J Struct Geol* 23:1727–1739
- Bassett KN, Busby CJ (2005) Tectonic setting of the Glimmer Conglomerate along the Sawmill Canyon fault zone, southern Arizona: a sequence analysis of an intra-arc strike-slip basin. In: Anderson TH, Nourse JA, McKee JW, Steiner MB (eds) *The Mojave-Sonora megashield hypothesis: development, assessment, and alternatives*. *Geol Soc Am Spec Pap* 393:377–400
- Beddoe-Stephens B, Millward D (2000) Very densely welded, rheomorphic ignimbrites of homogeneous intermediate calc-alkaline composition from the English Lake District. *Geol Mag* 137:155–173
- Bellier O, Sebrier M (1994) Relationship between tectonism and volcanism along the Great Sumatran fault zone deduced by SPOT image analyses. *Tectonophysics* 233:215–231
- Bellier O, Bellon H, Sebrier M, Sutanto MRC (1999) K-Ar age of the Ranau tuffs; implications for the Ranau Caldera emplacement and slip-partitioning in Sumatra (Indonesia). *Tectonophysics* 312:347–359
- Branney MJ, Kokelaar P (1992) A reappraisal of ignimbrite emplacement; progressive aggradation and changes from particulate to non-particulate flow during emplacement of high-grade ignimbrite. *Bull Volcanol* 54:504–520
- Branney MJ, Kokelaar P (1994) Volcanotectonic faulting, soft-state deformation and rheomorphism of tuffs during development of a piecemeal caldera. *Geol Soc Am Bull* 106:507–530
- Bryan SE, Cas RAF, Marti J (2000) The 0.57 Ma plinian eruption of the Granadilla Member, Tenerife (Canary Islands): an example of complexity in eruption dynamics and evolution. *J Volcanol Geotherm Res* 103:209–238
- Burkhardt B, Self S (1985) Extension and rotation of crustal blocks in northern Central America and effect on the volcanic arc. *Geology* 13:22–26
- Busby-Spera CJ (1988) Speculative tectonic model for the early Mesozoic arc of the southwest Cordilleran United States. *Geology* 16:1121–1125
- Busby CJ, Bassett K, Steiner MB, Riggs NR (2005) Climatic and tectonic controls on Jurassic intra-arc basins related to northward drift of North America. In: Anderson TH, Nourse JA, McKee JW, Steiner MB (eds) *The Mojave-Sonora megashield hypothesis: development, assessment, and alternatives*. *Geol Soc Am Spec Pap* 393:359–376
- Camus G, Gorgaud A, Moussand-Berthommier P-C, Vincent P-M (2000) Merapi (Central Java, Indonesia): An outline of the structural and magmological evolution, with a special emphasis to the major pyroclastic events. *J Volcanol Geotherm Res* 100:139–163
- Cashman KV, Thornber C, Kauahikaua JP (1999) Cooling and crystallization of lava in open channels and the transition of pahoehoe lava to a'a. *Bull Volcanol* 61:306–323
- Cashman KV, Sturtevant B, Papale P, Navon O (2000) Magmatic fragmentation. In: Sigurdsson H, Houghton BF, McNutt SR, Rymer H, Stix J (eds) *Encyclopedia of volcanoes*. Academic, New York, pp 421–430
- Cembrano J, Herve F, Lavenu A (1996) The Liquine Ofqui fault zone: a long lived intra-arc fault system in southern Chile. *Tectonophysics* 259:55–66
- Chesner CA (1998) Petrogenesis of the Toba Tuffs, Sumatra, Indonesia. *J Petrol* 39:397–438
- Christie-Blick N, Biddle KT (1985) Deformation and basin formation along strike-slip faults. In: Biddle KT, Christie-Blick N (eds) *Strike-slip deformation, basin formation and sedimentation*. *SEPM Spec Pub* 37:1–34
- Cioni R, Sbrana A, Vecci R (1992) Morphological features of juvenile pyroclasts from magmatic and phreatomagmatic deposits of Vesuvius. *J Volcanol Geotherm Res* 51:61–78
- Cioni R, Marianelli P, Santacroce R, Sbrana A (2000) Plinian and subplinian eruptions. In: Sigurdsson H, Houghton BF, McNutt SR, Rymer H, Stix J (eds) *Encyclopedia of volcanoes*. Academic, New York, pp 477–494
- Cole JW, Lewis KB (1981) Evolution of the Taupo-Hikurangi subduction system. *Tectonophysics* 72:1–21
- Collinson JD (1996) Alluvial sediments. In: Reading HG (ed) *Sedimentary environments: processes, facies and stratigraphy*. Blackwell Science, Oxford, pp 37–82
- Cowan H, Pettinga JR (1992) Late quaternary tectonics and landscape evolution Glynn Wye, North Canterbury, Field Trip Guides, Joint Annual Conf Geol Soc New Zealand and New Zealand Geophys Soc, Geological Society of New Zealand Misc Pub 63B:51–73
- Cowan HA, Pettinga JR, Smith IEM (1989) Transension and structural complexity along the Hope Fault, Glynn Wye to Hammer Basin, North Canterbury. *Geol Soc New Zealand Misc Pub* 43:31
- Crowell JC (1974) Origin of late Cenozoic basins in southern California. In: *Tectonics and sedimentation*, *SEPM Spec Pub* 22, Tulsa, OK, USA, pp 190–204
- Crowell JC (1982) The tectonics of Ridge basin, southern California. In: Crowell JC, Link MH (eds) *Geologic history of Ridge basin southern California*: *SEPM Series book* 22, Pac Sec pp 25–41
- De Rita D, Giordano G, Esposito A, Fabbri M, Rodani S (2002) Large volume phreatomagmatic ignimbrites from the Colli Albani volcano (Middle Pleistocene, Italy). *J Volcanol Geotherm Res* 118:77–98
- Dewey JF (1980) Episodicity, sequence, and style at convergent plate boundaries. In: Strangway DW (ed) *The continental crust and its mineral deposits*. *Geol Assoc Canada Spec Pap* 20:533–573
- Drewes H (1971) Geologic map of the Mount Wrightson Quadrangle, southeast of Tucson, Santa Cruz and Pima Counties, Arizona. *US Geol Surv Map* I-614
- Druitt TH, Sparks SJ (1981) A proximal ignimbrite breccia facies on Santorini, Greece. *J Volcanol Geotherm Res* 13:147–171
- Druitt TH, Young SR, Baptie B, Bonadonna C, Calder ES, Clarke, AB, Cole PD, Harford CL, Herd RA, Luckett R, Ryan G, Voight B

- (2002) Episodes of cyclic Vulcanian explosive activity with fountain collapse at Soufriere Hills Volcano, Montserrat. In: Druitt TH, Kokelaar BP (eds) The eruption of Soufriere Hills Volcano, Montserrat, from 1995 to 1999. *Geol Soc London Mem* 21:281–306
- Fierstein J, Houghton BF, Wilson CJN, Hildreth W (1997) Complexities of plinian fall deposition at vent: an example from the 1912 Novarupta eruption (Alaska). *J Volcanol Geotherm Res* 76:215–227
- Fink JH, Anderson SW (2000) Lava domes and coulees. In: Sigurdsson H, Houghton BF, McNutt SR, Rymer H, Stix J (eds) *Encyclopedia of volcanoes*. Academic, New York, pp 307–320
- Fisher RV, Schmincke HU (1984) *Pyroclastic rocks*. Springer, New York
- Fisher RV, Smith A, Roobol MJ (1980) Destruction of St Pierre, Martinique, by ash-cloud surge, May 8 and 20, 1902. *Geology* 8:472–476
- Fitch TJ (1972) Plate convergence, transcurrent faults, and internal deformation adjacent to southeast Asia and the western Pacific. *J Geophys Res* 77:4432–4460
- Francis P (1993) *Volcanoes: A planetary perspective*. Clarendon, Oxford
- Freundt A (1999) Formation of high-grade ignimbrites Part II. A pyroclastic suspension current model with implications also for low-grade ignimbrites. *Bull Volcanol* 60:545–567
- Freundt A, Wilson CJN, Carey SN (2000) Ignimbrites and block-and-ash flow deposits. In: Sigurdsson H, Houghton BF, McNutt SR, Rymer H, Stix J (eds) *Encyclopedia of volcanoes*. Academic, New York, pp 581–600
- Geist EL, Childs JR, Scholl DW (1988) The origin of summit basins of the Aleutian Ridge: implications for block rotation of an arc massif. *Tectonics* 7:327–341
- Gioncada A, Mazzuoli R, Bisson M, Pareschi MT (2003) Petrology of volcanic products younger than 42 ka on the Lipari-Vulcano complex (Aeolian Islands, Italy): an example of volcanism controlled by tectonics. *J Volcanol Geotherm Res* 122:191–220
- Giordano G, De Rita D, Cas, Rodani S (2002) Valley pond and ignimbrite veneer deposited in the small-volume phreatomagmatic “Perino Ibano” basic ignimbrite, Lago Albano maar, Colli Albani volcano, Italy: influence of topography. *J Volcanol Geotherm Res* 118:131–144
- Gourgaud A, Thouret J-C, Bourdier J-L (1988) Stratigraphy and textural characteristics of the 1982–1983 tephra of Galunggung volcano (Indonesia): implications for volcanic hazards. *J Volcanol Geotherm Res* 104:169–186
- Heiken G, Wohletz G (1985) *Volcanic ash*. University of California Press, Berkeley
- Henry CD, Wolff JA (1992) Distinguishing strongly rheomorphic tuffs from extensive silicic lavas. *Bull Volcanol* 54:171–186
- Holdsworth RE, Strachan RA, Dewey JF (1998) Continental transpressional and transtensional tectonics. *Geol Soc London Spec Pub* 135
- Hon K, Gansecki C, Kauhikaua J (2002) The transition from a’a to pahoehoe crust on flows emplaced during the Pu’u O-o - Kupaianaha eruption. In: Heliker C, Swanson DA, Takahashi TJ (eds) *The Pu’u O-o - Kupaianaha eruption of Kilauea volcano*. U.S. Geol Surv Prof Pap 1676:89–104
- Houghton BF, Wilson CJN, Pyle DM (2000a) Pyroclastic fall deposits. In: Sigurdsson H, Houghton BF, McNutt SR, Rymer H, Stix J (eds) *Encyclopedia of volcanoes*. Academic, New York, pp 555–570
- Houghton BF, Wilson CJN, Smith RT, Gilbert JS (2000b) Phreatoplinian eruptions. In: Sigurdsson H, Houghton BF, McNutt SR, Rymer H, Stix J (eds) *Encyclopedia of volcanoes*. Academic, New York, pp 513–526
- Israde-Alcantara I, Garduno-Monroy VH (1999) Lacustrine record in a volcanic intra-arc setting: the evolution of the Late Neogene Cuitzeo basin system (central-western Mexico, Michoacan). *Palaeogeog Palaeoclim Palaeoecol* 151:209–227
- Jarrard RD (1986a) Relations among subduction parameters. *Rev Geophys* 24:217–284
- Jarrard RD (1986b) Terrane motion by strike-slip faulting of forearc slivers. *Geology* 14:780–783
- Jurado-Chichay Z, Walker GP (2001) Variability of plinian fall deposits: examples from Okataina Volcanic Centre, New Zealand. *J Volcanol Geotherm Res* 111:239–263
- Kirsten LA, Hawkesworth CJ, Garland FG (2001) Felsic lavas or rheomorphic ignimbrites: is there a chemical distinction? *Contrib Mineral Petrol* 142:309–322
- Klute MA (1991) *Sedimentology, sandstone petrofacies, and tectonic setting of the Late Mesozoic Bisbee Basin, southeastern Arizona*. PhD thesis, University of Arizona, Tucson
- Larsen JF, Nye CJ, Ray LA (2000) The 2050 BP Okmok caldera forming event: evidence for magma mixing as an eruption trigger. *EOS Trans AGU* 81, Fall Meet Suppl, F2000
- Lawton TF, McMillan J (1999) Arc abandonment as a cause for passive continental rifting: comparison of the Jurassic Mexican Borderland rift and the Cenozoic Rio Grande rift. *Geology* 27:779–782
- Link M (2003) Depositional systems and sedimentary facies of the Mio-Pliocene Ridge Basin group, Ridge Basin, California. In: Crowell JC (ed) *Evolution of Ridge Basin, southern California: an interplay of sedimentation and tectonics*. *Geol Soc America Spec Pap* 367:17–88
- McCaffrey R (1992) Oblique plate convergence, slip vectors, and forearc deformation. *J Geophys Res* 97:8905–8915
- McCurry M, Schmidt K (2001) Petrology and oxygen isotope geochemistry of the Pucon Ignimbrite–Southern Andean Volcanic Zone, Chile: implications for genesis of mafic ignimbrites. III South Am Symp Isotope Geol, Abstr, Soc Geol de Chile, Santiago, Chile, pp 317–320
- McCurry M, Watkins K, Parker J, Wright K, Hughes S (1996) Preliminary volcanological constraints for sources of high-grade, rheomorphic ignimbrites of the Cassia Mountains, Idaho: implications for the evolution of the Twin Falls volcanic center. In: Hughes S, Thomas R (eds), 21<sup>st</sup> Annual Field Conference of the Tobacco Root Geological Society, Twin Falls. *Northwest Geol* 26:81–91
- McPhie J, Doyle M, Allen R (1993) *Volcanic textures: a guide to the interpretation of textures in volcanic rocks*. Center for Ore Deposit and Exploration Studies, University of Tasmania
- Melson WG, Saenz R (1973) Volume, energy, and cyclicity of eruptions of Arenal volcano, Costa Rica. *Bull Volcanol* 37:416–437
- Milner SC, Duncan AR, Ewart AD (1992) Quartz latite rheoignimbrite flows of the Etendeka Formation, northwestern Namibia. *Bull Volcanol* 54:200–219
- Miyabuchi Y (1999) Deposits associated with the 1990–1995 eruption of Unzen Volcano, Japan. *J Volcanol Geotherm Res* 89:139–158
- Morrissey M, Mastin LG (2000) Vulcanian eruptions. In: Sigurdsson H, Houghton BF, McNutt SR, Rymer H, Stix J (eds) *Encyclopedia of volcanoes*. Academic, New York, 463–476
- Morrissey M, Zimanowski B, Wohletz K, Buettner R (2000) Phreatomagmatic fragmentation. In: Sigurdsson H, Houghton BF, McNutt SR, Rymer H, Stix J (eds) *Encyclopedia of volcanoes*. Academic, New York, pp 431–446
- Nairn IA, Self S (1978) Explosive eruptions and pyroclastic avalanches from Ngauruhoe in February 1975. *J Volcanol Geotherm Res* 3:39–60
- Nakada S, Shimizu H, Ohta K (1999) Overview of the 1990–1995 eruption at Unzen Volcano. *J Volcanol Geotherm Res* 89:1–22
- Nilsen TH, Sylvester AG (1995) Strike-slip basins. In: Busby CJ, Ingersoll RV (eds) *Tectonics of sedimentary basins*. Blackwell Science, Cambridge, MA, pp 425–457
- Reineck HE, Singh IB (1980) *Depositional sedimentary environments*, 2nd ed. Springer, Berlin
- Riggs NR, Busby-Spera CJ (1990) Evolution of a multi-vent volcanic complex within a subsiding arc graben depression: Mount Wrightson Formation, Arizona. *Geol Soc Am Bull* 102:1114–1135

- Ryan H, Coleman PJ (1992) Composite transform-convergent plate boundaries: description and discussion. *Mar Petrol Geol* 9:89–97
- Sarewitz DR, Lewis SD (1991) The Marinduque intra-arc basin, Philippines: basin genesis and in situ ophiolite development in a strike-slip setting. *Geol Soc Am Bull* 103:597–614
- Schmincke H-U, Swanson D (1967) Laminar viscous flowage structures in ash-flow tuffs from Gran Canaria, Canary islands. *J Geol* 75:641–644
- Self S (1983) Large scale phreatomagmatic silicic volcanism: a case study from New Zealand. *J Volcanol and Geotherm Res* 17:433–469
- Self S, Sparks RSJ (1978) Characteristics of widespread pyroclastic deposits formed by the interaction of silicic magma and water. *Bull Volcanol* 41:196–212
- Self S, Wilson L, Nairn IA (1979) Vulcanian eruption mechanisms. *Nature* 277:440–443
- Self S, Thordarson T, Keszthelyi L (1997) Emplacement of continental flood basalt lava flows. In: Mahoney JJ, Coffin MF (eds) *Large igneous provinces: continental, oceanic and planetary flood volcanism*. Am Geophys Union, Geophys Monograph 100:381–410
- Sigurdsson H, Houghton B, McNutt SR, Rymer H, Stix J (eds) (2000) *Encyclopedia of volcanoes*. Academic, Boston
- Smith GA, Landis CA (1995) Intra-arc basins. In: Busby CJ, Ingersoll RV (eds) *Tectonics of sedimentary basins*. Blackwell Science 263–298
- Smith GA, Lowe DR (1991) Lahars: Volcano-hydrologic events and deposition in the debris flow-hyperconcentrated flood flow continuum. In Fisher RV, Smith GA (eds) *Sedimentation in volcanic settings*. SEPM Spec Pub 45:59–70
- Smith RT, Houghton BF (1995) Vent migration and changing eruptive style during the 1800a Taupo eruption: new evidence from the Hatepe and Rotongaio pheatoplinian ashes. *Bull Volcanol* 57:432–439
- Sparks RSJ (1997) Causes and consequences of pressurization in lava dome eruptions. *Earth Planet Sci Lett* 150:177–189
- Sparks RSJ, Self S, Walker GPL (1973) Products of ignimbrite eruptions. *Geology* 1:115–118
- Stix J, Torres CR, Navarez ML, Cortes JGP, Raigosa AJ, Gomez MD, Castonguay R (1997) A model of vulcanian eruptions at Galeras volcano, Colombia. *J Volcanol Geotherm Res* 77:285–303
- Thomson SN (2002) Late Cenozoic geomorphic and tectonic evolution of the Patagonian Andes between latitudes 42°S and 46°S: An appraisal based on fission-track results from the transpressional intra-arc Liquine-Ofqui fault zone. *Geol Soc Am Bull* 114:1159–1173
- Ui T, Matsuwo N, Sumita M, Fujinawa A (1999) Generation of block and ash flows during the 1990–1995 eruption of Unzen Volcano, Japan. *J Volcanol Geotherm Res* 89:123–137
- Vallance JW (2000) Lahars. In: Sigurdsson H, Houghton BF, McNutt SR, Rymer H, Stix J (eds) *Encyclopedia of volcanoes*. Academic, New York, pp 601–616
- Van Dijk JP (1994) Late Neogene kinematics of intra-arc oblique shear zones: the Petilia-Rizzuto fault Zone (Calabrian arc, central Mediterranean). *Tectonics* 13:1201–1230
- Ventura G (1994) Tectonics, structural evolution and caldera formation on Vulcano Island (Aeolian Archipelago, southern Tyrrhenian Sea). *J Volcanol Geotherm Res* 60:207–224
- Walker GPL (1981) Plinian eruptions and their products. *Bull Volcanol* 44:223–240
- Weinberg RF (1992) Neotectonic development of western Nicaragua. *Tectonics* 11:1010–1017
- Wilson L (1980) Relationships between pressure, volatile content and ejecta velocity in three types of volcanic explosion. *Jour Volcanol Geoth Res* 8:297–313
- Wilson CJN, Houghton B, McWilliams MO, Lanphere M, Weaver SD, Briggs RM (1995) Volcanic and structural evolution of Taupo Volcanic Zone, New Zealand; a review. *J Volcanol Geotherm Res* 68:1–28
- Wohletz K (1986) Explosive magma-water interactions: thermodynamics, explosion mechanisms, and field studies. *Bull Volcanol* 48:245–264
- Wolff JA, Wright JV (1981) Rheomorphism of welded tuffs. *J Volcanol Geotherm Res* 10:13–34
- Wood RA, Pettinga JR, Bannister S, Lamarche G, McMorran TJ (1994) Structure of the Hanmer strike-slip basin, Hope Fault, New Zealand. *Geol Soc Am Bull* 106:1459–1473
- Yamagishi H, Freerbreyc C (1995) Ballistic ejecta from the 1988–1989 andesitic Vulcanian eruptions of Tokachidake volcano, Japan: morphological features and genesis. *J Volcanol Geotherm Res* 59:269–278